

A SOIL GENESIS INVESTIGATION INTO POSSIBLE LONG-RANGE TRANSPORT
OF FOREIGN SEDIMENTS IN THE STANN CREEK DISTRICT OF BELIZE

by

Heath R. A. Sawyer

A Thesis Presented to

The Faculty of Humboldt State University

In Partial Fulfillment of the Requirements for the Degree

Master of Science in Environmental Systems: Geology

Committee Membership

Dr. Mark A. Hemphill-Haley, Committee Chair

Dr. Raymond 'Bud' Burke, Committee Member

Dr. Brandon E. Schwab, Committee Member

Dr. Margaret Lang, Program Graduate Coordinator

December 2019

ABSTRACT

A SOIL GENESIS INVESTIGATION INTO POSSIBLE LONG-RANGE TRANSPORT OF FOREIGN SEDIMENTS IN THE STANN CREEK DISTRICT OF BELIZE

Heath R. A. Sawyer

Throughout the world, long range transport (LRT) of aeolian dust plays a major role in the total global dust budget. Research suggests that LRT dust from the deserts of north Africa play a role in soil genesis in the Americas. The focus of this study is a preliminary investigation for evidence of north African dust or volcanic ash influence on the soils in the Cockscomb Basin Wildlife Sanctuary in Stann Creek District, Belize. A series of 7 soil profiles were analyzed from a catena transect to determine if there is evidence of foreign materials by using X-ray diffraction and Scanning Electron Microscope analyses in order to identify mineralogy and micro-abrasions that would indicate parent material origin from a possible influence of LRT dust. This yielded the finding that there is little convincing evidence for LRT dust deposition in the soils examined.

ACKNOWLEDGMENTS

I would first like to thank my loyal field partner, Mitch Danforth. Without his efforts, hard work, dedication to soil science and willingness to leave his life for five months to live in a Belizean jungle, this project would have never taken place. I would also like to acknowledge my complete and undying gratitude to my mentor, Bud Burke. His encouragement, support, and unwavering dedication to my overall success helped me to complete this project. I thank Dr. Joy Winbourne, for demonstrating and helping teach me about jungle research. Without her, unknowingly taking me under her wing, I would have not felt comfortable conducting jungle research on my own. She is a constant source of knowledge and inspiration and for that I am internally grateful.

I am forever thankful to Fred Fisher, he supported, financed and had the knowledge and creativity to create the opportunity for this study to take place. I am extremely grateful to Jen and Mac McDougal. They generously provided a safe house for us to stay, maintain a proper storage area for all my field-based needs and logistical support while in Belize. Much appreciation goes out to the Belizean Audubon Society and the rangers of the Cockscomb Basin Wildlife Sanctuary. Their generosity, jungle knowledge and friendship contributed to making this experience a success.

I specifically thank each of my committee members Dr. Mark Hemphill-Haley, Dr. Brandon Schwab, and Joseph Seney for their critical review and encouragement to complete this thesis.

Special thanks to Nathan Graham and Zackery Seama for their assistance and enthusiasm in my final field work expedition. Special thanks also to Ronna Bowers and Diane Sutherland for their technical assistance, knowledge and support in writing this thesis.

My sincere appreciation to Dr. Benjamin Z. Houlton and Dr. Randall Southard for their input and use of laboratory analysis equipment at U.C. Davis.

Last but definitely not least, this is for my parents, Beau and Kathleen Sawyer. Your love and unwavering support have taken me to the ends of the earth and back. I thank you from the bottom of my heart.

TABLE OF CONTENTS

ABSTRACT.....	ii
ACKNOWLEDGMENTS	iii
TABLE OF CONTENTS.....	v
LIST OF FIGURES	vii
LIST OF APPENDICES.....	ix
INTRODUCTION	1
Study Location	5
Previous Research	8
Purpose and Scope.....	9
REGIONAL SETTING	10
Geology and Structure.....	10
Soils	14
Vegetation & Disturbance History	15
Climate	16
METHODS	17
Fieldwork.....	19
Laboratory Methods	22
Particle size distribution analysis.....	22
X-ray diffraction analysis	22
FEI Quanta 250 Scanning Electron Microscope.....	23

RESULTS	25
Particle Size Distribution.....	25
Clay Mineralogy.....	25
Scanning Electron Microscope.....	29
DISCUSSION.....	33
CONCLUSIONS.....	38
REFERENCES	40
APPENDIX A: WIND DIRECTION	50
APPENDIX B: PARTICLE SIZE DISTRIBUTION ANALYSIS PROCEDURE.....	62
APPENDIX C: SOIL DESCRIPTION AND LABORATORY DATA.....	64
APPENDIX D: PEDON PROFILE PARTICLE SIZE DISTRIBUTION.....	71
APPENDIX E: X-RAY DIFFRACTION ANALYSIS GRAPHS.....	73
APPENDIX F: SCANNING ELECTRON MICROSCOPE PHOTOMICROGRAPHS PLATES	80

LIST OF FIGURES

Figure 1. Regional map illustrating study sites for this and previous LRT dust studies. ...	4
Figure 2. Map of global setting representing location of Belize. https://www.mapsofworld.com/belize/maps/location-map-of-belize.jpg	6
Figure 3. Study area within the Cockscomb Basin Wildlife Sanctuary (CBWS), Belize. .	7
Figure 4. Study area is within the Cockscomb Basin Wildlife Sanctuary, Stann Creek District, Belize.	8
Figure 5. Geological regional map of Belize. Black arrow pointing to the Cockscomb Basin Wildlife Sanctuary. Figure modified from Meerman, (2008). http://belizeinfocenter.org/geology-101-for-belizean-students-and-investors/	11
Figure 6. Geologic time scale of the Maya Mountains, Belize. Figure modified from Bates and Hall, (1977).	13
Figure 7. The field study area approximately 11.4 km ² plot located west of the Cockscomb Basin Wildlife Sanctuary Ranger Station. Pedon locations along the transect are numbered one through seven from top of the slope to the floodplain. ..	18
Figure 8. Example of a pedon profile. Horizon designations are identified by red and white pins.	21
Figure 9. XRD diffractogram from Pedon 4 (Backslope), B horizon (39-100 cm) representing primary clay mineralogy of kaolinite.	26

Figure 10. XRD trace from Pedon 6 (Flood Plain), C horizon (62-100 cm). representing dominant clay mineralogy of kaolinite and illite. 28

Figure 11. Pedon 3, A horizon, 0-22 cm, centered in figure is a silt size (quartz?) grain, mostly angular, with sharp corners and edges, and shows conchoidal fractures, grain size ~50 μm in width. Grain is sitting on a matrix of kaolinite honeycomb micro-structure..... 30

Figure 12. Pedon 1, A horizon, 0-9 cm, centered in figure is a silt size (quartz?) grain, mostly angular, with sharp corners and edges, and shows conchoidal fractures, grain size ~30 μm in width. Grain is sitting on a matrix kaolinite honeycomb micro-structure..... 31

Figure 13. Pedon 4, A horizon, 0-6 cm, centered in figure is a silt size (quartz?) grain, mostly sub-angular, with rounded corners and edges, exhibiting possible conchoidal fractures, possible chatter marks, grain size ~40 μm in width. Grain is sitting on a matrix of kaolinite clay particles interbedded in a kaolinite honeycomb micro-structure..... 32

Figure 14. NASA composition map from June 28, 2018, illustrating the expansive dust plumes stretching from the Sahara, Sahel region of north African to Central America, Belize is highlighted..... 36

LIST OF APPENDICES

APPENDIX A: WIND DIRECTION	50
APPENDIX B: PARTICLE SIZE DISTRIBUTION ANALYSIS PROCEDURE.....	62
APPENDIX C: SOIL DESCRIPTIONS AND LABORATORY DATA.....	64
APPENDIX D: PEDON PROFILE PARTICLE SIZE DISTRIBUTION.....	71
APPENDIX E: X-RAY DIFFRACTION ANALYSIS GRAPHS.....	73
APPENDIX F: SCANNING ELECTRON MICROSCOPE PHOTOMICROGRAPHS PLATES	80

INTRODUCTION

Long-range transport (LRT) of dust (aerosols) has gained major attention over the past several decades: its various far-reaching impacts on climatic processes (Harrison et al., 2001; Evan et al., 2009; Knippertz et al., 2017); ocean and terrestrial biogeochemical cycles (Jickells et al., 2005; Mahowald et al., 2008; Shao et al., 2011), and human and ecosystem health (Prospero et al., 2005; Griffin, 2007; Prospero et al., 2014). The corresponding impact dust may have on land, atmosphere, and ocean systems depends upon particle physiochemical characteristics such as mineralogy, morphology, and particle size distribution (Mahowald et al., 2011; Zhang et al., 2016). These physiochemical characteristics are a trait derived from the parent source and can be subject to modification during transport (Mahowald et al., 2011; Zhang et al., 2016). Alteration during LRT, is most notably due to the loss of large particles and the transition of the particle size scale to smaller sizes and chemical processing (“aging”) during transit (Usher et al., 2003; Prather et al., 2008; Prospero et al., 2013).

LRT dust can bring nutrients, critical in helping sustain vegetation in regions with naturally depleted soils (Swap et al., 1992). Mineralogy of LRT dust contains small amounts of iron (3.5%) and other elements, which fertilize and provide micronutrient for the world’s oceans. (Martin et al., 1991; Muhs et al., 2007; Mahowald et al., 2011). LRT dust inputs into terrestrial biogeochemical cycles, such as nutrient depleted subtropical and tropical soils can influence both nutrient-holding capacity and nutrient status of these

ecosystems. An example of this is the significant contribution of LRT dust to soil formation throughout the Caribbean, Bahamas, and Americas (Muhs et al., 2013), bringing with it vital nutrients such as phosphorus and molybdenum that contribute to soil fertility (Swap et al., 1992; Muhs et al., 2013; Prospero et al., 2013). Additionally, LRT dust can affect the global climate by altering the earth's radiation budget due to absorption and scattering of incoming solar radiation and outgoing long-wave radiation (Harrison et al., 2001).

The largest producers of aeolian dust in the world are the Sahara and Sahel regions of North Africa (Figure 1; Prospero et al., 2013) producing ~240 to 1600 Tg yr⁻¹ of mineral aerosols (Prospero et al., 2002; Engelstaedter et al., 2006). This represents 70% of the global total, and is six times larger than the second largest aeolian source in Asia (Liu et al., 2011; Prospero et al., 2013). North African dust has been found as far north as the Alps and Pyrenees in Europe, in the form of “red snows,” however, this phenomenon is sporadic (Prospero et al., 1981). In contrast, the LRT of mineral aerosols into the North Atlantic is annual and often produces a widespread thick haze (Prospero et al., 1981). The trans-Atlantic transport of the north-easterly trade winds can carry dust from North Africa, west across the Atlantic towards the Americas. During the boreal summer and fall (April to October) dust transport occurs at high altitude “Sahara Air Layer,” reaching 5-6 km in height, when the intertropical convergence zone moves north (Caquineau et al., 2002). These winds can transport dust from Africa as far northwest as Rocky Mountain National Park in Colorado, and as far north as Acadia National Park in

Maine (Perry et al., 1997). In boreal winter months (November to April) as winds shift, dust is transported in the trade wind layer at an altitude of 1.5-3 km and has been found as far south as the Amazon Rainforest in Brazil (Caquineau et al., 2002; Yu et al., 2015).

The significance of LRT dust to the genesis of soils on limestone islands in the western Atlantic Ocean and Caribbean Sea has been emphasized by multiple studies. In the Bahamas, Syers et al. (1969), Foos (1991), and Carew and Mylroie (1991) all suggest, the clay rich soils are primarily derived from African dust. Herwitz et al. (1996) conclude that African dust largely contributed to the red, clay-rich character of Bermuda's red soils. Muhs et al. (1990) suggest that African dust is the primary source for soils on Barbados, Jamaica, the Bahamas, and the Florida Keys. Muhs and Budahn (2009) suggest a secondary source of the clay-rich soils developed on Quaternary reef terraces of Barbados is likely from volcanic ash originating from the Lesser Antilles. While the majority of the LRT dust research has been conducted on pure limestone islands in the western Atlantic Ocean and Caribbean Sea, little to no research has been conducted on the Central America mainland (Figure 1).

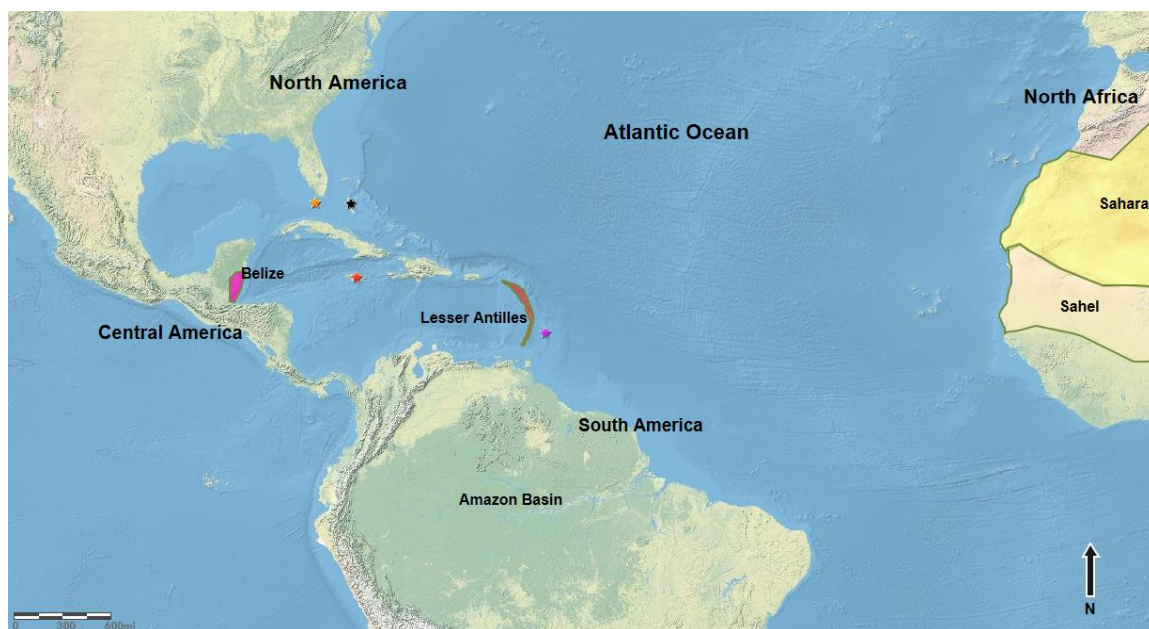


Figure 1. Regional map (North America, Central America, South America, Atlantic Ocean, North Africa) illustrating study sites for this and previous long range transport dust studies. Previous studies are denoted by stars.

Atmospheric Saharan dust sampling identified the primary mineral aerosols as a mixture of quartz, feldspars, and clays, sometimes associated with calcite and/or palygorskite (Caquineau et al., 2002). Studies of clay rich soils conducted on high purity limestone islands (Barbados, the Florida Keys, and the Bahamas) in the western Atlantic and Caribbean Sea concluded that quartz is the most abundant mineral in the silt size fraction, and mica dominates the clay size fraction (Muhs et al., 2009). In smaller quantities, kaolinite, chlorite, microcline, plagioclase, calcite, and gypsum are also present (Muhs et al., 2009).

Prior studies throughout the Americas and the Caribbean have documented dust deposits having mineralogic composition derived from parent materials of Sahara/Sahel region in north Africa, or the Lesser Antilles volcanic arc system (Carey and Sigurdsson, 1980; Middleton and Goudie, 2001; Muhs et al., 2007; Ben-Ami et al., 2010; Yu et al., 2015). However, there have been few studies published on soils of Central Belize, and no investigation into the potential eolian inputs in this region.

The objectives of this pedological investigation are: (1) to determine the presence of potential LRT dust in south central Belize; (2) if apparently present, to describe the physical, chemical, and mineralogical properties of the LRT dust, and (3) to determine whether the origin of the dust deposits is the Sahara/Sahel region of north Africa or ash from volcanic eruptions in the Lesser Antilles (Figure 1). In order to test for the presence of LRT dust, I sampled soils in the Cockscomb Basin Wildlife Sanctuary from a watershed with well-documented biotite-rich granitic parent materials catena transect.

Study Location

Belize is located along the northeastern coast of Central America, between 15°45′ - 18°30′N and -87°30′ - 89°15′W, on the Yucatán Peninsula (Figure 2). Belize has an area of 22,960 km², about 9,500 km² of which are protected areas. One of these protected sites is the Cockscomb Basin Wildlife Sanctuary (CBWS). The CBWS is the focal point of this study and located in south central Belize, on the east-facing slopes of the Maya Mountains (16°42′58.32" N and -88°39′38.88" W), approximately 15 km from the

Caribbean coastline, Stann Creek District, and covers an area of approximately 400 km² of tropical forest, with an approximate elevation of 50 m to 1,120 m (Victoria Peak) above sea level (Figure 3).

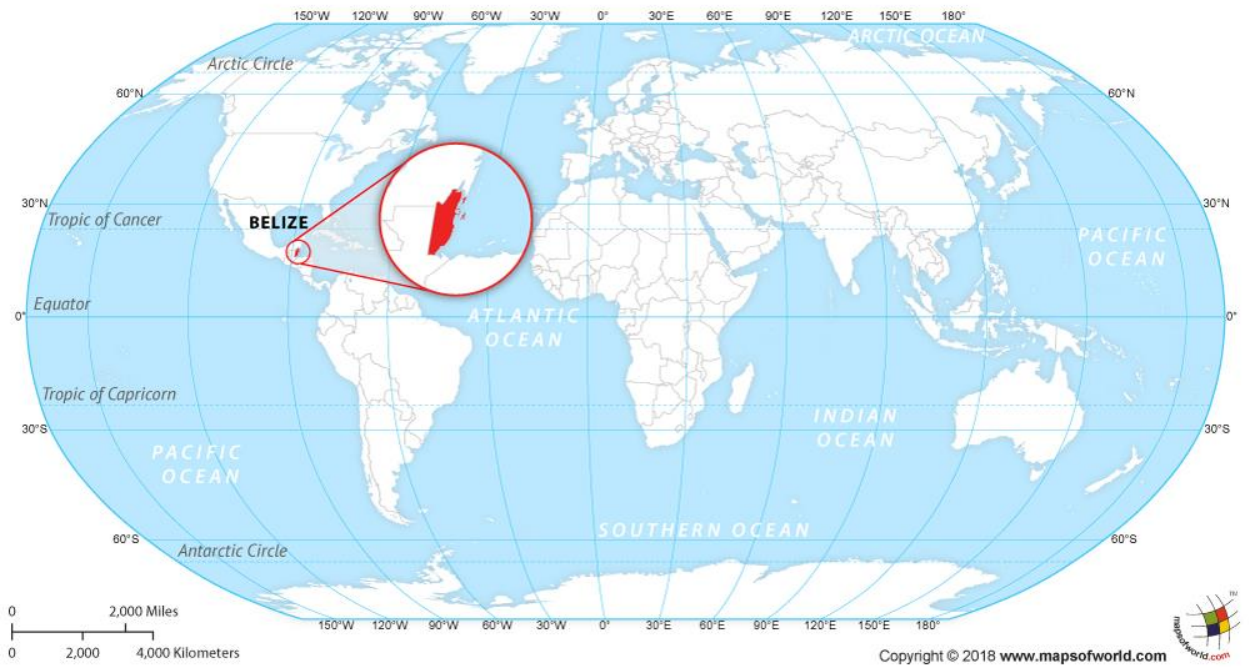


Figure 2. Map of global setting representing location of Belize.
<https://www.mapsofworld.com/belize/maps/location-map-of-belize.jpg>



Figure 3. Map of Central America indicating location of Belize in relation to Mexico, Guatemala and Honduras. Also illustrated, study area of the Cockscomb Basin Wildlife Sanctuary (CBWS) within the Maya Mountains, Belize.

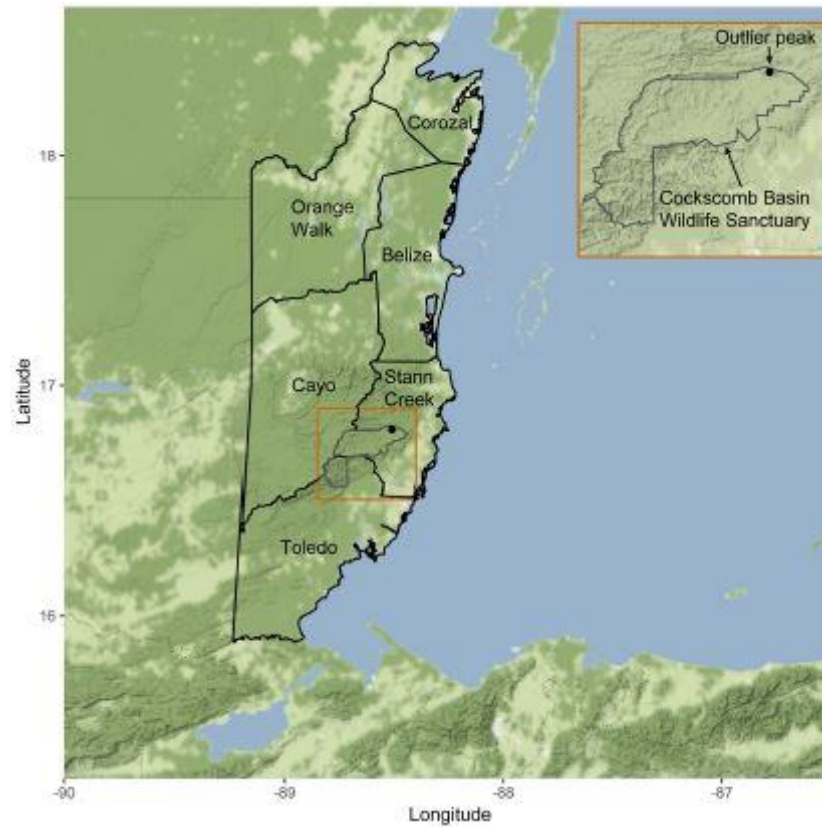


Figure 4. Map of Belize, illustrating the districts of Belize and where the Cockscomb Basin Wildlife Sanctuary is located within Stann Creek District, Belize. Figure modified from Holst (2019).

Previous Research

Published regional geologic and soil maps provided limited local source data on the CBWS. Only three major geology-soil-vegetation-land use studies have been conducted in Belize.

The British Honduras Provisional Soil Map of Write et al., (1959) examined the soils and associated vegetation of the entire country. The second study, Geology of the

Maya Mountains (Bateson and Hall, 1977) is a bibliographical reference investigating the physical features of the Maya Mountains of Belize. This includes the history of previous observations made by travelers and scientists of the Maya Mountains since the end of the 19th century. These historical accounts help build the basic geologic map of central Belize. The third study (King et al., 1989) is a survey conducted to update the land suitability assessment of Stann Creek District, Belize which was used to aid agricultural developmental based on soil classification and land use of the area.

Purpose and Scope

The focus of this study is to establish whether there is LRT dust playing a role in the soil genesis of the Cockscomb Basin Wildlife Sanctuary, Stann Creek District of Belize. This includes: 1) identify land form, position on landform and parent material; 2) describe soil profiles; 3) collect samples for analysis; 4) conduct lab analysis (X-ray diffraction); 5) interpret micro morphological abrasions of clay and silt size particles using the scanning electron microscope (SEM).

REGIONAL SETTING

Geology and Structure

The overall structure of the Belizian Maya Mountains is that of an uplifted fault block that has gone through multiple orogenic periods (Dixon, 1956; Bateson and Hall, 1977). There is evidence for an orogeny that deformed the Maya Mountain Block (MMB) during the late Permian and early Triassic time periods (Bateson, 1972; Bateson et al., 1977; Cole and Andrews-Jones, 1979). The Maya Mountains consist of fault bounded highlands (<1200 m elevation) that are composed of variably metamorphosed sediments intruded by a number of mineralogically similar granitic intrusions (Bateson et al., 1977). Bateson and Hall (1977) describe this isolated mountain block of sediments and volcanic rocks as comprised of one geologic group that extended in time from the Pennsylvanian to approximately the middle Permian, that were intruded by granitic rocks during the early Triassic (Kesler et al., 1974) (Figure 5).

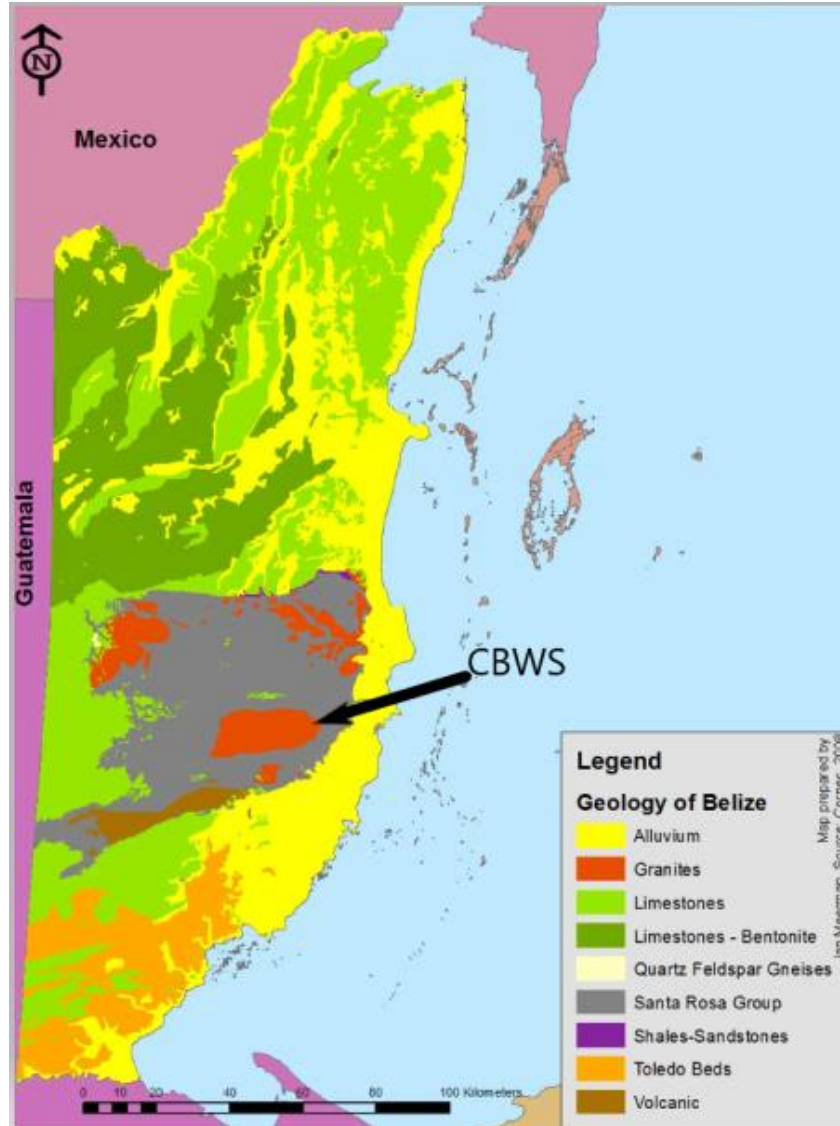


Figure 5. Geological regional map of Belize. Black arrow pointing to the Cockscomb Basin Wildlife Sanctuary (CBWS). Figure modified from Meerman, (2008). <http://belizeinfocenter.org/geology-101-for-belizean-students-and-investors/>

The modern horst structure of the MMB is thought to have initiated during the Mid-Cretaceous, although major regional lineaments were inherited from features of at least the Paleozoic age (McBirney, 1969). From Middle Cretaceous to Middle Tertiary time the MMB was flanked by the Northern and Southern Boundary Fault Zones and subject to periodic relative uplift (Bateson et al., 1977). Other than the boundary fault zones, the MMB has been cut by multiple faults, some of which have been found in the Cockscomb Basin (Bateson, 1977).

The Cockscomb Basin is composed of Lower Pennsylvanian intrusive igneous rock, the Cockscomb-Sapote Granite. Cockscomb-Sapote granite is a two-mica bearing granite, with high amounts of biotite. A mixture of feldspars consists of some microcline, orthoclase, and smaller plagioclase crystals with a composition near the oligoclase-andesine boundary (Bateson et al., 1977). Quartz is also found in sufficient quantity for the rock to be classified as granite (Bateson et al., 1977). Other parent material found within the CBWS consists of the Upper Pennsylvanian to Middle Permian Santa Rosa Group (sediment and metasediment), and a Cretaceous limestone capping the extreme western mountain tops surrounding the basin (Bateson et al., 1977) (Figure 5).

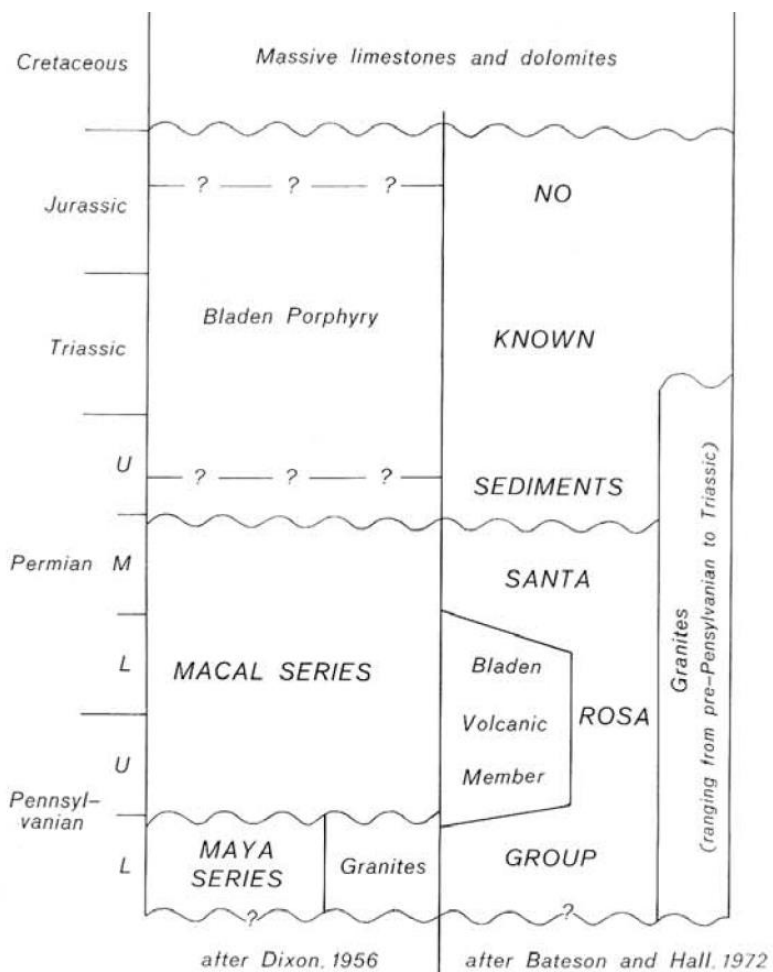


Figure 6. Geologic time scale of the Maya Mountains, Belize. Figure modified from Bates and Hall, (1977).

Soils

Soils in the eastern Cockscomb Basin are primarily derived from granitic rocks and various sedimentary rocks including limestone. Steep uplands flow into a broad valley. The flood plain soils are characteristically deeper (> 150 cm to bedrock) with acidity levels ranging from approximately 5.0 to 7.0 pH (Baillie et al., 1993). Physical and chemical weathering processes that have occurred over millennia throughout the basin, have leached most of the major cations and plant nutrients out of the system producing highly weathered soils (Baillie et al., 1993). Primary minerals, such as feldspars and micas, have weathered to secondary clay minerals, such as kaolinite and illite (Weil and Brady, 2017). Removal of ions such as magnesium, iron, and potassium through hydrolysis, dissolution, acid reactions, and oxidation/ reduction can destabilize the crystalline structure of primary minerals. These soluble cations and silicic acids can recombine to form clay minerals, or be lost from the weathering environment to ground water (Weil and Brady, 2017).

CBWS Modern Fluvial System

CBWS is divided approximately in half, into two well-defined watersheds. The western side drains to the Monkey River, and the eastern side to South Stann Creek. The study area is located in the headwaters of the upper South Stann Creek watershed. South Stann Creek meanders east, across a relatively flat, broad basin, with 75% of the area

lying below 200 m (Kamstra, 1987). The South Stann Creek watershed is covered by an intricate dendritic stream and creek patterns (Kamstra, 1987).

Vegetation & Disturbance History

Much of Cockscombs basin is vegetated, secondary forest growth that has undergone multiple periods of logging between the end of World War II and the late 1980's (Kamstra, 1987). Several hurricanes, including Abby (1960), Hattie (1961), Fifi (1974), Greta (1978), Mitch (1998), and Iris (2001) (Avila, 2001; Pielke, et al., 2003; McCloskey and Keller, 2009) have also affected vegetation patterns and forest regrowth.

Vegetation within the study area is classified as a broad-leaf forest, consisting of a diverse mix of evergreen with some semi-evergreen tropical hardwood species (Kamstra, 1987). One of the most dominant species in the east basin is the cohune palm (*Attalea cohune*), occupying about 80 percent of the basin and growing primarily below 200 m in elevation (Kamstra, 1987). Other co-dominant species include iron wood (*Dialium guianense*), quamwood (*Schizolobium parakybum*), negrito (*Simauruba glauca*), prickly yellow (*Zasnthoxylum kellermanii*), polewood (*Xylopiia frutescens*), and yemeri (*Vockysia hondurensis*) (Kamstra, 1987). The structure and species composition of the forest varies across the basin with changes in parent material (mineralogy), precipitation, topography (slope & relief), and time (age of vegetation since human occupation) (Jenny, 1941; Kamstra, 1987).

Climate

Belize's weather is characterized by two seasons, rainy and dry. The rain season occurs primarily during the months of June thru December/January. Annual rainfall ranges variably from northern to southern Belize. The northern lowlands and central inland areas of Belize are subtropical, while southern Belize, including the Maya Mountains, lie in the Inter-Tropical Convergence Zone. This, and orographic precipitation, enhances rainfall activity in the Cockscomb Basin. The CBWS is classified as tropical wet seasonal (Walsh, 1996), with an approximate annual rainfall of 1829 – 3810 mm (~72 – 150 in) and a dry season from February to May. Temperatures range approximately 11-39 °C (52 – 102 °F) with a mean daily temperature of ~25°C (Cockscomb Basin Wildlife Sanctuary Management Plan, 2005-2010).

Annual wind data are based on observations taken between 02/2004 – 10/2019, and were collected from the International Airport in Ladyville, Belize. Prevailing wind direction is offshore (easterly trade winds) during the months of February-September, while wind direction fluctuates from the northeast to north-northeast during the months of October-January. Refer to Appendix A for more detailed wind graphs (<https://www.windfinder.com/windstatistics/belize>).

METHODS

The study area for this project is an approximately 11.4 km² plot located west of the CBWS ranger station (Figure 3). During the dry season from February to June, 2013, my field assistant and I dug and described to a depth of 1 meter. Seven of the 42 pits were chosen for more detailed investigation of presence of aeolian inputs, and located along a transect orientated north-south along the western edge of the 11.4 km² plot (Figure 7). The transect was chosen to represent all slope positions from summit to toeslope, and is located as far as possible from roads, the ranger station, visitor center, and other infrastructure in order to limit anthropogenic soil disturbance. The catena transect location was developed on a single rock type (granitic) to simplify identification of non-parent material clay mineralogy and to maximize laboratory analysis by limiting the of soil profiles to seven pits within the transect.

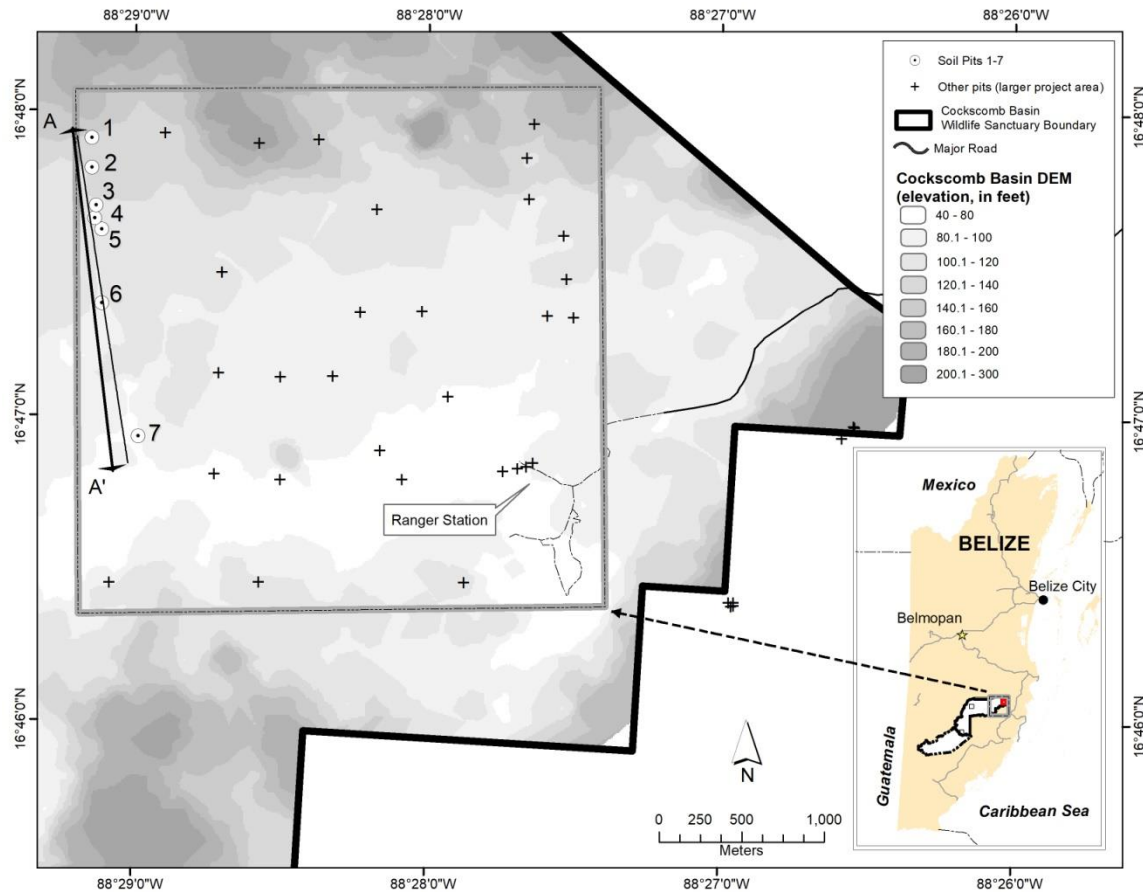


Figure 7. Map of the field study area approximately 11.4 km² plot located west of the Cockscomb Basin Wildlife Sanctuary Ranger Station. Pedon locations along the transect are numbered one through seven from top of the slope to the floodplain.

Fieldwork

In order to test for the presence of LRT dust inputs, I sampled soils derived from granitic parent material (colluvium and residuum) across a catena. A soil catena is ideally investigated on soils with homogenous parent material, physical, chemical and textural characteristics as well as similar uniform climatic regime (Birkeland, 1999). The catena transect featured five hillslope positions (Birkeland, 1999): identified in Figure 6: (1) summit, (2) shoulder, (3) backslope, (4) foot slope, and (5) toe slope. For this study two additional pedons were investigated along the catena transect, in the flood plain (6 & 7). These positions provide a snapshot of soil genesis and associated slope processes.

Morphological soil development, possible aeolian influence, and forest vegetation change significantly with age and slope position (Birkeland, 1999). Slope relief and slope angle were difficult to quantify in the field due to dense vegetation growth, making visibility very difficult and hand-held GPS satellite reconnaissance virtually unreliable.

Pre-trip site selection planning included use of the best available topographic map (a 100-m cell size DEM) to select the target transect area. Tropical jungle vegetation and steep, undulating terrain, and presence of jaguars, pumas, and fer-de-lance in the field areas presented significant challenges to pit site selection, and field mapping in general. Even with copious use of our machetes, visibility was typically <10 feet. The proximate spacing of the middle three profile pits (3-4-5) was due to access limitations.

We dug each pit to a depth of at least 1-meter and 1-meter wide unless restricted by a lithic or para-lithic contact (Table 1). We identified horizons and soil depth, and documented soil color, field estimated percent sand, silt and clay, assigned texture class, structure, and clay films and presence of carbonate. Each soil horizon was then measured, described, photographed (Figure 8), and a 1-gallon volume of soil material was sampled using the Field Book for Describing and Sampling Soils, Version 3.0 (USDA, 2012). Sampled soils were left to air dry prior to transport and storage. Pits were located using a handheld Garmin GPSmap 62s and backfilled before leaving each site.

The soil data collected in the investigation were used to analyze for potential LRT dust in the soils of the CBWS. It should be noted, the pedon description presented in Appendix C, are not to be used as formal USDA soil descriptions of the Cockscomb Basin.



Figure 8. Example of a pedon profile. Horizon designations are identified by red and white pins.

Laboratory Methods

Particle size distribution analysis

I conducted particle size distribution analysis (PSD) on soil samples collected to determine sand, silt and clay fractions of each horizon. Results were used to correlate with field estimates and to obtain the fine-grained clay and silt fraction (<0.06 mm) that would contain possible evidence of LRT dust (Muhs, et al., 2007).

Summary of procedure; bulk samples were air-dried, and coarse grained material removed from samples by dry sieving through a series of different standard sieve sizes (3/4 in, No. 4, No. 10, No. 40, No. 200). PSD was determined on all fine-grained (<No. 200 sieve) transect samples by pipette method after removal of organic matter with hydrogen peroxide and dispersion with sodium hexametaphosphate (Singer and Janitzky, 1986). Full procedure is outlined in Appendix B.

X-ray diffraction analysis

In order to further study the pedogenesis of the catena transect and the possible influence of LRT dust, I conducted an x-ray diffraction analysis (XRD) on the clay fraction (<0.002 mm) from each horizon along the catena transect. Using a Rigaku Ultima IV X-Ray Diffractometer at University of California, Davis, I analyzed the clay

size fraction by collecting distinct x-ray diffraction patterns to identify clay mineralogy based on d-spacing.

For each horizon I prepared four samples for analysis. During PSD, 25 ml of suspended clay solution was collected from each horizon (25 horizons) and allowed to settle out of solution. Four glass slides were prepared by mounting the clay slurry from each of the 25 samples on the slide and allowed to dry and then treated in one of four ways: air dry; glycol hydration bath; heated at 350 °C; and heated at 550 °C. X-ray diffractograms were collected on each of the four slides and superimposed on the same plot (Appendix E). Changes in d-spacing was compared between each of the four treatments. Identification of mineral species was based on techniques outlined in the methods of Carroll (1970).

FEI Quanta 250 Scanning Electron Microscope

High-resolution secondary electron photomicrographs of silt and clay size particles were produced using the FEI Quanta 250 Scanning Electron Microscope (SEM) at Humboldt State University. The photomicrographs show mineral grain morphology. The morphology of LRT quartz grains can be identified by well-rounded grains, numerous surficial percussion pits, scratches, non-oriented v-shaped pitting, and fractured edges (Khalaf and Gharib, 1985; Mazzullo et al., 1986; Smith et al., 2001).

Several steps were taken to obtain these images. A 25ml sample of the fine-grained fraction (silt and clay) from the A horizons of pedons 1-5 were collected during PSD, added to distilled water, and diluted to a ratio of 1:10. A 1.27 cm double sided sticky carbon tape was placed against a half inch SEM aluminum sample stub. A piece of micro-pore filter paper was then placed against the sticky tape. One to two drops of 1:10 solution was added to the micro-paper using a micro-pipette, and placed in desiccator to dry. The sample was then gold coated, using a Denton Desk II Gold Coater, and purged with Argon gas. SEM secondary electron images were then produced from each of the gold coated samples to detect and interpret possible micro-geomorphic windblown abrasion structures, that may indicate LRT dust.

The five A horizons analyzed during this study were chosen due to their location on the catena, (1) summit, (2) shoulder, (3) backslope, (4) foot slope, (5) toe slope. Pedon locations six and seven were not analyzed due to their location in the flood plain.

RESULTS

Particle Size Distribution

PSD analysis was used to adjust field estimates of sand, silt, and clay and to assign soil texture class. Soil texture classes ranged from sandy loam to silty clay (see, Appendices C & D).

Due to historical logging within the CBWS, PSD was used to interpret slope pedogenesis stability. Tropical soils are formed in regions of high annual temperature and rainfall with rapid, intense weathering leading to mature clay rich soils (Young, 1980; Gupta, 2011). Laboratory PSD analysis of pedon soil textures, indicate a relatively young soils with a predominately sandy loam to loam textures throughout the transect, (see, Appendix C). The possible catena soil-geomorphology field pedon observation logs are presented in Appendix D.

Clay Mineralogy

I investigated the pedogenesis of the transect and the possible influence of LRT dust by conducting a XRD analysis on the clay fraction (<0.002 mm) from each pedon horizon along the transect. The dominant clay mineralogy identified along the catena

landscape was Kaolinite, $\text{Al}_2\text{Si}_2\text{O}_5(\text{OH})_4$. Kaolinite is a secondary clay mineral chemically weathered from feldspars. Kaolinite formation is consistent with both local granitic parent material and LRT dust from North Africa.

In figure 9, I present XRD diffractogram from this study. It illustrates the unique set of 2 theta peak patterns that can be used to identify kaolinite. Kaolinite peaks can be observed at $\sim 7.15^\circ$ 2 theta (001), and $\sim 3.75^\circ$ 2 theta (002). These peaks stay consistent through glycolation and at 350°C treatment, and become amorphous when heated to 550°C . Identification of mineral species was based on techniques outlined in the methods of Carroll (1970).

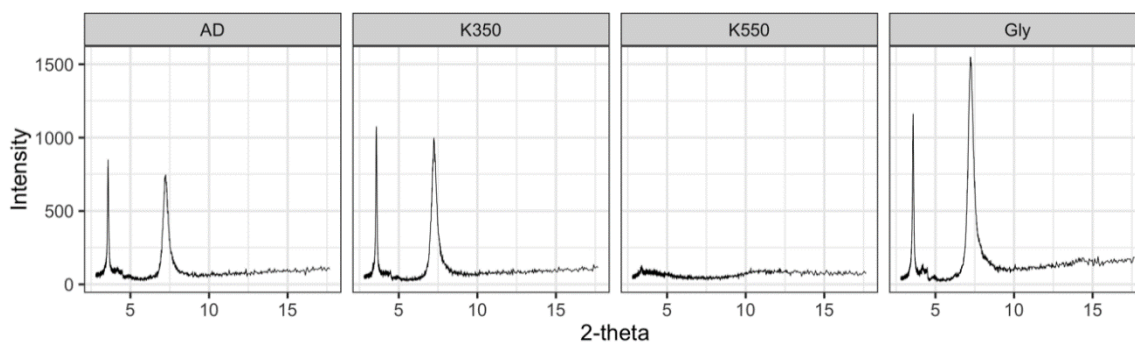


Figure 9. Examples of XRD diffractogram which represents the primary clay mineralogy of Kaolinite. This sample is from the B horizon of the footslope position (Pedin 4 at depth 39-100 cm). The y-axis shows intensity. The x-axis shows 2-theta. Changes in intensity along 2-theta was compared between each of the four treatments: air died (AD), 350°C (K350), 550°C (K550) and glycolation (Gly) to identify clay mineralogy.

A second clay mineral, Illite, $(K,H_3O)(Al,Mg,Fe)_2(Si,Al)_4O_{10}[(OH)_2,(H_2O)]$ was also in pedons six and seven. Illite is a secondary clay mineral chemically weathered from feldspars. Illite formation is consistent with both local granitic parent material and LRT dust from North Africa.

In Figure 7, I present an XRD diffractogram from this study. It illustrates the unique set of 2 theta peak patterns that can be used to identify illite. Illite peaks can be characterized by the presence of $\sim 10.11^\circ$ 2 theta (001), $\sim 5.02^\circ$ 2 theta (002), and $\sim 3.33^\circ$ 2 theta (003) at air dried condition. Sample heated to 350°C , shows minimal to no change, $\sim 10.02^\circ$ 2 theta (001), $\sim 5.00^\circ$ 2 theta (002), and $\sim 3.33^\circ$ 2 theta (003). Sample treated with glycol, no change is observed, $\sim 10.02^\circ$ 2 theta (001), $\sim 5.00^\circ$ 2 theta (002), and $\sim 3.33^\circ$ 2 theta (003). Sample heated to 550°C , $\sim 10.02^\circ$ 2 theta (001), $\sim 4.98^\circ$ 2 theta (002), and $\sim 3.33^\circ$ 2 theta (003). Identification of mineral species was based on techniques outlined in the methods of Carroll (1970). The full set of diffractograms from this study can be found Appendix E.

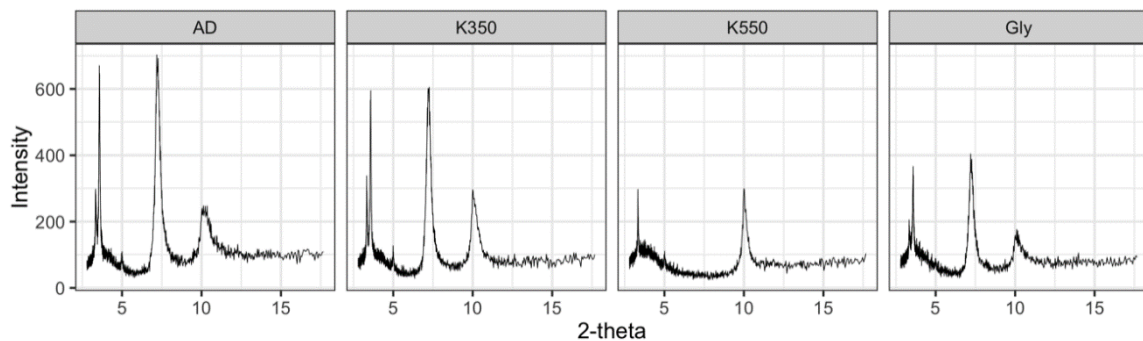


Figure 10. Examples of XRD diffractogram which represents the primary clay mineralogy of Kaolinite. This sample is from the C horizon of the floodplain - 1 position (Pedon 6 at depth 62-100 cm). The y-axis shows intensity. The x-axis shows 2-theta. The y-axis shows intensity. The x-axis shows 2-theta. Changes in intensity along 2-theta was compared between each of the four treatments: air died (AD), 350 °C (K350), 550 °C (K550) and glycolation (Gly) to identify clay mineralogy.

XRD analysis was inconclusive. Kaolinite and illite are both secondary clay minerals chemically weathered from feldspars that are consistent with both local granitic parent material and LRT dust.

Scanning Electron Microscope

High-resolution secondary electron photomicrographs of silt and clay size particles were produced using the SEM at Humboldt State University. No quartz grain particles that were imaged were positively identified to exhibit physical morphological features characteristic of LRT (e.g. well-rounded grains, numerous surficial percussion pits, scratches, none-orientated v-shaped pitting, and fractured edges). Multiple images of clay structure, and fine-grained rock fragments were interpreted in the imagery. Most rock fragments identified in the secondary electron photomicrographs exhibited sharp angular corners and little to no abrasion marks (Figures 11, 12, and 13). Figure 13 is the only grain from this study that exhibits subangular features and what may be interpreted as micro abrasions, but not conclusive of LRT.

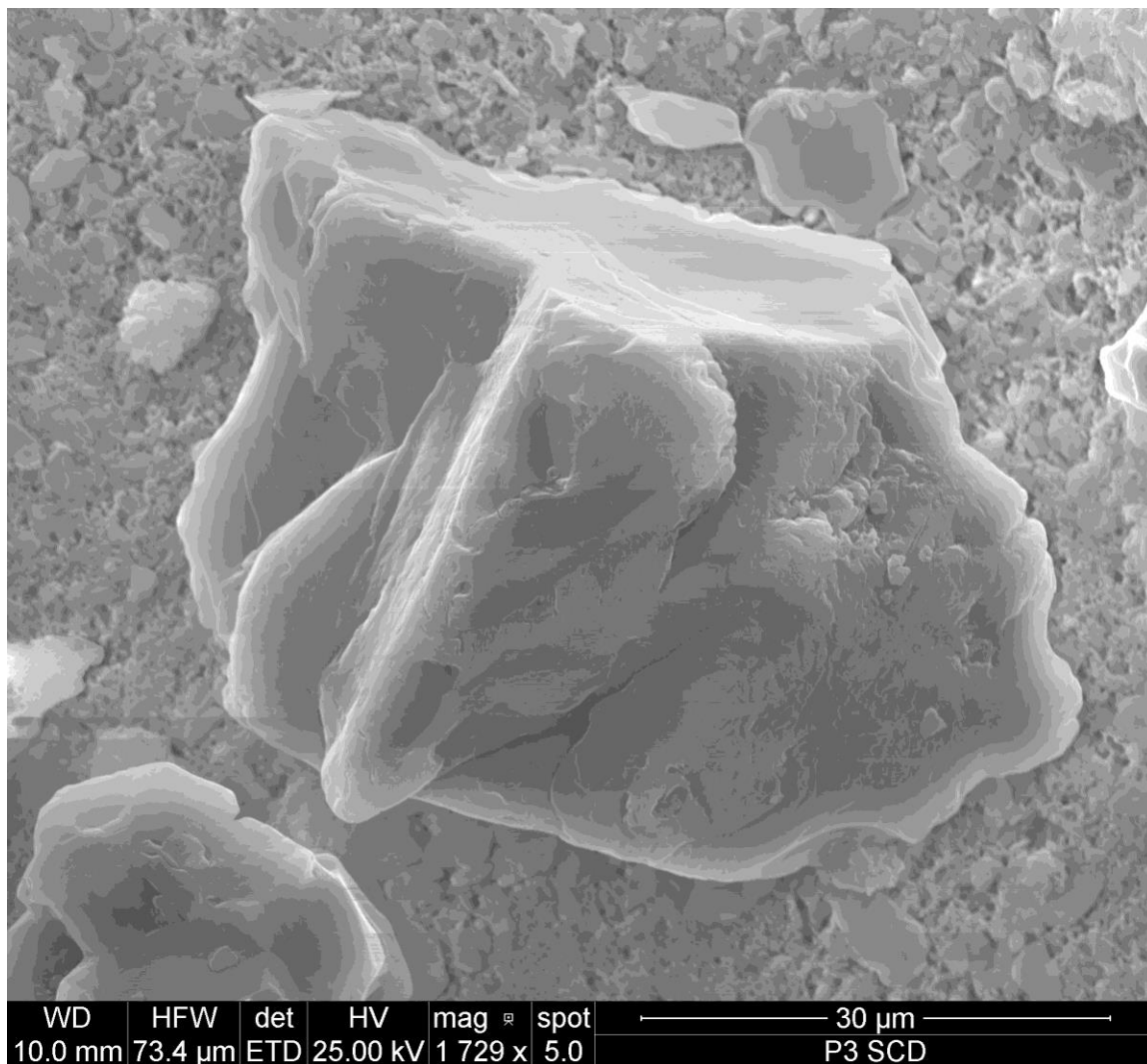


Figure 11. Pedon 3, A horizon, 0-22 cm, centered in figure is a silt size (quartz?) grain, mostly angular, with sharp corners and edges, and shows conchoidal fractures, grain size ~50 μm in width. Grain is sitting on a matrix of kaolinite honeycomb micro-structure.

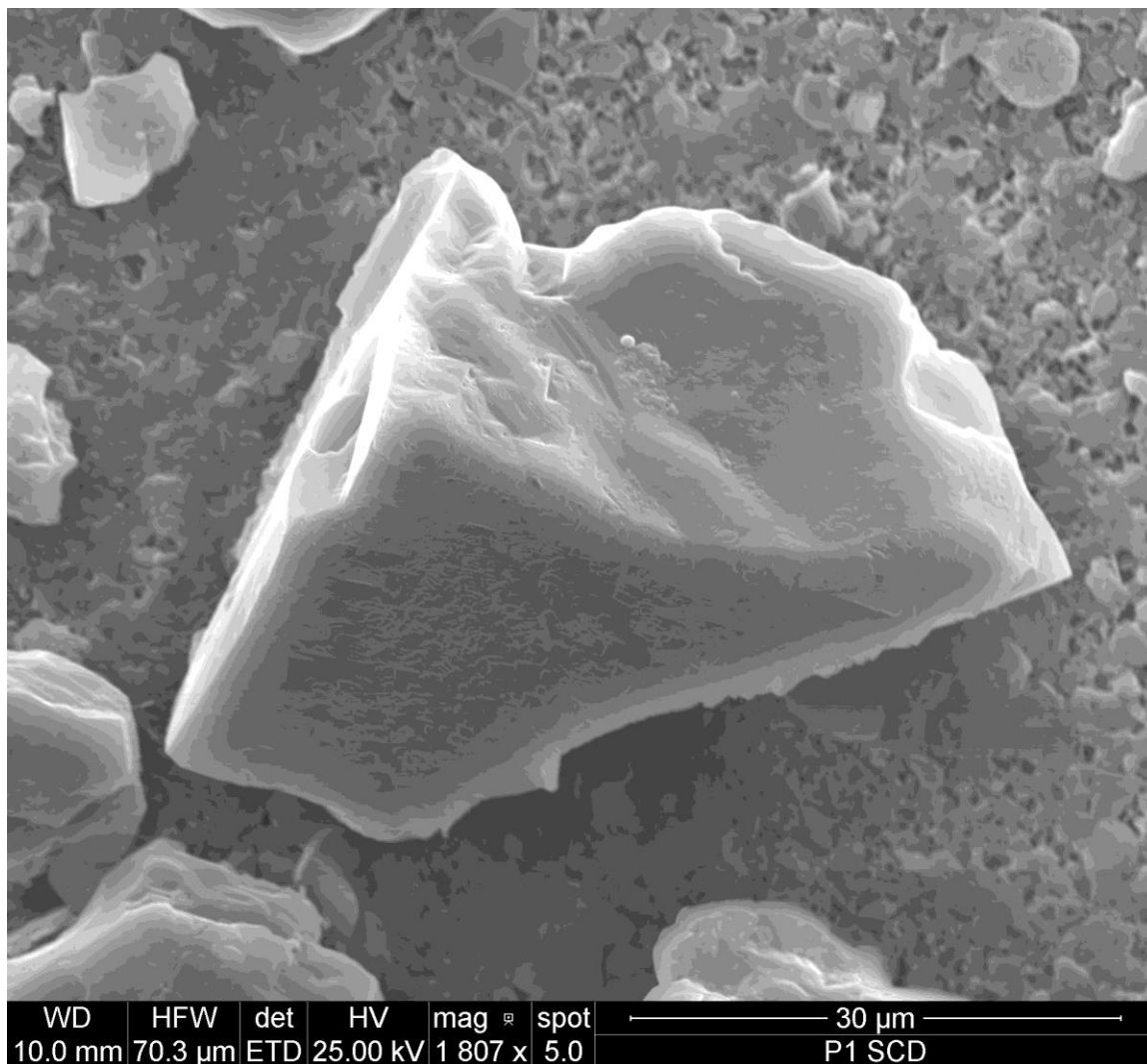


Figure 12. Pedon 1, A horizon, 0-9 cm, centered in figure is a silt size (quartz?) grain, mostly angular, with sharp corners and edges, and shows conchoidal fractures, grain size ~30 μm in width. Grain is sitting on a matrix kaolinite honeycomb micro-structure.

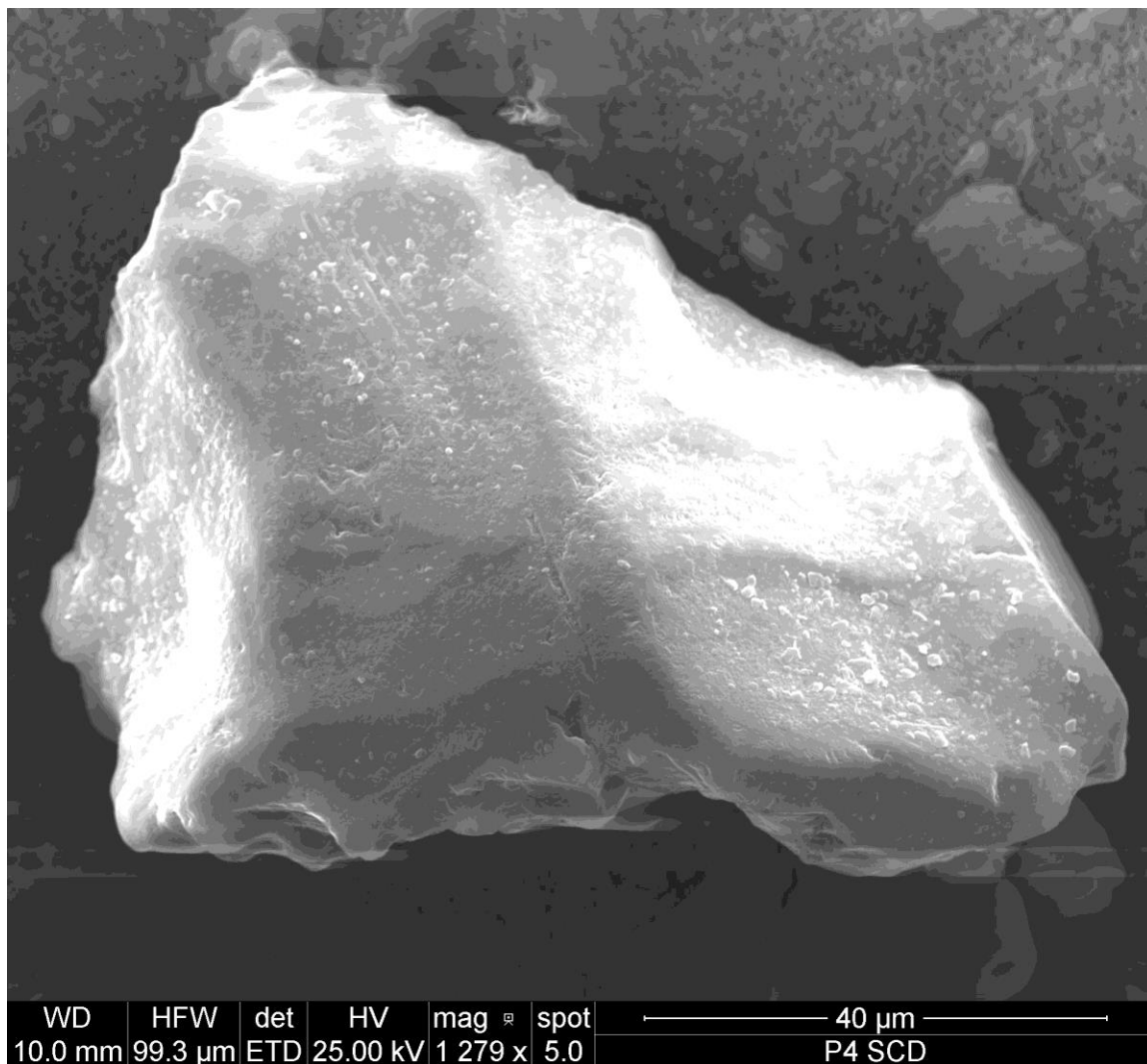


Figure 13. Pedon 4, A horizon, 0-6 cm, centered in figure is a silt size (quartz?) grain, mostly sub-angular, with rounded corners and edges, exhibiting possible conchoidal fractures, possible chatter marks, grain size $\sim 40 \mu\text{m}$ in width. Grain is sitting on a matrix of kaolinite clay particles interbedded in a kaolinite honeycomb micro-structure.

To view Scanning Electron Microscope images not presented in the results chapter, please refer to Appendix G.

DISCUSSION

The main objective of this research was to detect LRT dust in the CBWS, Stann Creek District, Belize. Based on results of x-ray diffraction and scanning electron microscope analyses of clay mineralogy and structure of soils collected along the catena transect, I interpreted as a local parent material source (granitic) throughout the summit, shoulder, backslope, foot slope, toe slope. The humid, acidic conditions of CBWS accelerate the breakdown of the granitic parent material and increase the formation of secondary minerals, kaolinite and illite from weathering amphibole, biotite and plagioclase feldspar. Acidity is influenced by both rainfall and organic matter.

Evidence I expected to see if LRT dust was present in the soils of the CBWS, would be found in the fine grains fraction (silt and clay) and not a function of local parent material (granitic) pedogenesis. Well documented mineralogy associated with LRT dust are quartz, kaolinite, illite, smectite, chlorite, microcline, plagioclase, calcite and gypsum (Caquineau et al., 2002; Muhs et al., 2007). Using the XRD, I would look for mineralogically different evidence, it may come in the form of arid-land clays and precipitates like smectite and gypsum. Additionally, I would look for physical micro-abrasions on quartz grain from LRT and mechanical weathering processes. SEM evidence of this would be observed by well-rounded quartz grains, numerous surficial percussion pits, scratches, none-orientated v-shaped pitting, and fractured edges.

Other potential foreign LRT sources not derived from the tropical weathering of the CBWS granitic parent material might include volcanic ash from the Lesser Antilles Volcanic Arc or other nearby volcanic centers. The Lesser Antilles Volcanic Arc was often considered by other Caribbean researchers to be a possible source for pedogenesis within the region (Muhs et al., 2007). Arculus (1978) reported ash from the island of Granada was composed of variable proportions of olivine, magnetite, calcic augite, amphibole and plagioclase. Field samples, XRD and SEM analyses didn't render evidence of volcanic ash within the transect. This may be due to modern wind direction of the westerlies and lack of extremely explosive volcanic eruptions along the Lesser Antilles Volcanic Arc system within the last 30,000 years B.P. Any evidence of volcanic air fall may have been eroded by anthropogenic deforestation, erosional processes from annual rainfall, and bioturbation. Further discussion with petrologist Dr. Brandon Browne (personal communication, 2019) indicated preservation of volcanic ash in tropical environments is highly unlikely due to erosional processes.

Lack of interpreted LRT dust evidence in the CBWS is not due to a lack of potential source deposition. The largest global dust source in the world is the Sahara and Sahel regions of North Africa, with an annual estimated 240 to 1600 Tg of dust transported from the region, and 140 to 259 Tg carried and deposited across the Atlantic and Caribbean "dust belt" of 0–30° N (Das et al., 2013; Engelstaedter et al., 2006; Prospero et al., 1999). Despite being downwind of the largest global dust source, LRT

dust deposition in Belize have never been estimated, and contribution of LRT dust to the region is unknown. Observations from the Moderate Resolution Imaging Spectroradiometer (MODIS) on NASA's Terra satellite have indicated in late June, 2018 LRT of North African dust reached the Yucatán Peninsula, Guatemala and El Salvador, (Fig 11). Although, this is not a common annual occurrence; it is my opinion, this event may indicate a possible larger cyclical pattern that may bring vital nutrients from Africa to Central America.

Identification of LRT dust was inconclusive using methods outlined in this study. Although, kaolinite and illite are associated with soil genesis evidence of LRT dust on high-purity limestone islands in the north Atlantic and Caribbean Sea, the soil parent material on these islands are external to the carbonate substrate (Muhs et al., 2007). Allowing identification of LRT dust to be easily identified. Unlike the CBWS, were parent material (granitic) and LRT North African dust share some of the same clay identifiers. Factors that may have contributed to this outcome are, but not limited to site location, methodology and concentration, frequency and distance from parent source.

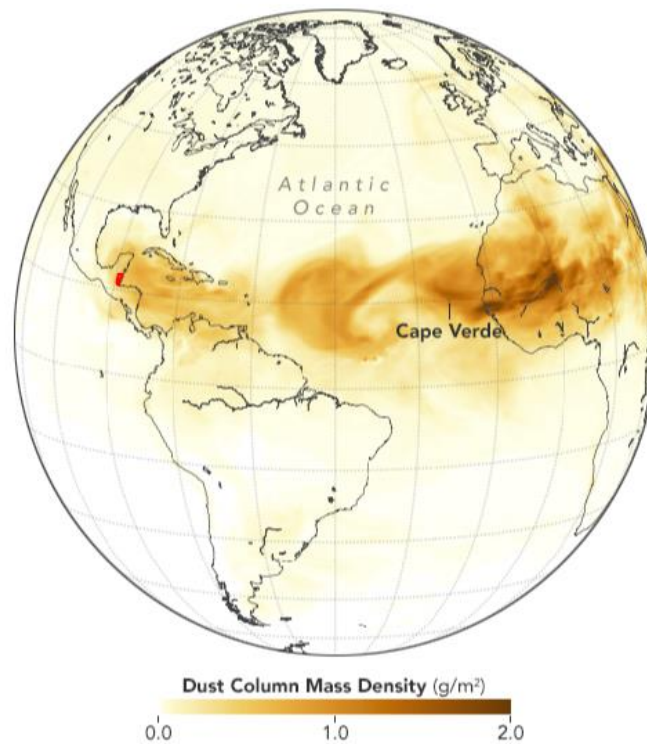


Figure 14. NASA composition map from June 28, 2018, illustrating the expansive dust plumes stretching from the Sahara, Sahel region of north African to Central America, Belize is highlighted in red.

<https://earthobservatory.nasa.gov/images/92358/here-comes-the-saharan-dust>

The lack of LRT dust in the Cockscomb region could be due to anthropogenic disturbances due to multiple periods of logging (Kamstra, 1987) that have transformed the physical environment, changing hydrology and geomorphology. Given the amount of annual rainfall the CBWS receives, once the vegetation protecting the soils was removed,

soil and regolith would have been de-structured (Gupta, 2011), an increase in erosion and sediment transfer would have happened very rapidly, taking with it any possibility of identifying a long-term LRT dust record.

This study represents the first LRT dust soil investigation on granitic parent material in the CBWS, Belize. NASA (2018), produced satellite imagery indicating a large pulse of LRT dust from North Africa stretching west ward across the Atlantic Ocean, Caribbean Sea and Central America (Fig. 11). This may indicate LRT dust from Africa maybe found in Belize.

Location of this investigation into possible LRT dust and methods used need to be reassessed and expanded on outside the CBWS. This is due to many decades of anthropogenic disturbances of pedogenesis through logging, mineralogical similarities of in situ weathering of locally-derived parent material with that of the LRT African dust and LRT dust activity occurring episodically in this region.

CONCLUSIONS

I participated in a soil genesis investigation along a 1.37- km long catena transect on a south-eastern facing slope in order to identify possible eolian deposition in a dense tropical secondary growth forest in the Cockscomb Basin Wildlife Sanctuary, Stann Creek District, Belize. I hand dug and profiled seven soil pits in this investigation, using standard soil description methods, I described seven soil profiles, documenting soil color, texture, structure, field clay percentages and collected samples for laboratory analysis.

X-ray diffraction and scanning electron microscope analyses of clay mineralogy and structure of soils collected along the catena transect have been interpreted as inconclusive. X-ray diffraction data has suggested, kaolinite to be the dominate mineralogy within the catena transect profile. Illite was also interpreted in two of the pedon profiles along the toe-slope. Kaolinite and illite, are consistent with clay minerals detected in LRT dust. However, local granitic parent material also weathers to secondary mineral precipitate, kaolinite and illite. Evidence I expected to see if North African LRT dust was present in the soils of the CBWS, would be found in the fine grains fraction (silt and clay) and not a function of local parent material (granitic) pedogenesis. I expected to find arid-land clays and precipitates like smectite and gypsum.

Scanning electron microscope analyses was also inconclusive. Multiple images of clay structure, fine-grained rock fragments and organic matter were observed in the

imagery. However, no well-rounded quartz grains with physical micro-abrasions from LRT, and mechanical weathering processes, were identified.

Another factor of to be considered, Cockscombs Basin has been anthropogenically altered due to multiple periods of logging (Kamstra, 1987) that have transformed the physical environment, changing hydrology and geomorphology (Kamstra, 1987). If future depositional history research is to be considered for a LRT dust, an anthropogenically unaltered environment should be studied.

REFERENCES

- Arculus, R.J., 1978, Mineralogy and petrology of Grenada, Lesser Antilles island arc. *Contributions to Mineralogy and Petrology*, 65(4), pp.413-424.
- Avila, L.A., 2001, Tropical Cyclone Report, Hurricane Iris, 4–9 October 2001. National Hurricane Center, 30.
- Baillie, I.C., Wright, A.C. S., Holder, M. A., and FitzPatrick, E. A., 1993, Revised Classification of the soils of Belize. NRI Bulletin 59. Chatham, UK: Natural Resource Institute.
- Bateson, J.H., 1972, New interpretation of geology of Maya Mountains, British Honduras. *AAPG Bulletin*, 56 (5), pp.956-963.
- Bateson, J.H., and Hall, I.H.S., 1977, Geology of the Maya Mountains. Institute of Geological Sciences, National Environment Research Counsel, Overseas Memoir 3.
- Ben-Ami, Y., Koren, I., Rudich, Y., Artexo, P., Martin, S.T., and Andreae, M.O., 2010, Transport of North African dust from the Bodé'lé depression to the Amazon Basin: a case study. *Atmos. Chem. Phys.*, 10, 7533–7544.
- Birkeland, P. W., 1999, *Soils and Geomorphology*. 3rd Edition, New York, Oxford, Oxford University Press, Inc.
- Caquineau, S., Gaudichet, A. L., Gomes, L., and Legrand, M., 2002, Mineralogy of Saharan dust transported over northwestern tropical Atlantic Ocean in relation to source regions. *J. Geophys. Res.*, 107(D15), 4251, doi:10.1029/2000JD000247.

- Carew, J.L., and Mylroie, J.E., 1991, Some pitfalls in paleosol interpretation in carbonate sequences. *Carbonates and Evaporites*, 6(1), p.69.
- Carey, S.N., and Sigurdsson, H., 1980, The Roseau ash: deep-sea tephra deposits from a major eruption on Dominica, Lesser Antilles arc. *Journal of Volcanology and Geothermal Research* 7, 67–86.
- Carroll, D., 1970, *Clay minerals: a guide to their X-ray identification* (Vol. 126). Geological Society of America.
- Cockscomb Basin Wildlife Sanctuary Management Plan 2005– 2010.
- Cole, G.L., and Andrews-Jones, D.A., 1978, Economic Evaluation of the Mineral Potential of Belize. An Overview of the Anschutz Mining Corporation Exploration Program in Belize, 1975-1977. Anchutz Mining Corporation. Third Annual Report, February.
- Dixon, C.G., 1955, *Geology of southern British Honduras, with notes on adjacent areas*: Belize Government Printer, 85 p.
- Engelstaedter, S., Tegen, I., and Washington, R., 2006, North African dust emissions and transport. *Earth-Science Reviews*, 79(1-2), pp.73-100.
- Evan, A.T., Vimont, D.T., Heidinger, A.K., Kossin, J.P., and Bennartz, R., 2009, The role of aerosols in the evolution of tropical North Atlantic Ocean temperature anomalies. *Science*, 324 (2009), pp. 778-781.
- Foos, A.M., 1991, Aluminous lateritic soils, Eleuthera, Bahamas; a modern analog to carbonate Paleosols. *Journal of Sedimentary Research*, 61(3), pp.340-348.

- Griffin, D.W., 2007, Atmospheric movement of microorganisms in clouds of desert dust and implications for human health. *Clinical microbiology reviews*, 20 (3), pp.459-477.
- Gupta, A., 2011, *Tropical geomorphology*. Cambridge University Press.
- Harrison, S.P., Kohfeld, K.E., Roelandt, C., and Claquin T., 2001, The role of dust in climate changes today, at the Last Glacial Maximum, and in the future. *Earth Sci. Rev.*, 54, 43–80.
- Herwitz, S.R., Muhs, D.R., Prospero, J.M., Mahan, S., and Vaughn, B., 1996, Origin of Bermuda's clay-rich Quaternary paleosols and their paleoclimatic significance. *Journal of Geophysical Research: Atmospheres*, 101(D18), pp.23389-23400.
- Holst, B.K., Gandy, E., Sallen, A., Amaya, D., Baron, E., Linares, A., and Bolon, B., 2019, Epiphytes and Lithophytes of Outlier, Stann Creek District, Belize. fieldguides.fieldmuseum.org, 1152, Version 1
- Jenny, H., 1941, *Factors of soil formation*. 281 pp. New York.
- Jickells, T.D., An, Z.S., Andersen, K.K., Baker, A.R., Bergametti, G., Brooks, N., Cao, J.J., Boyd, P.W., Duce, R.A., Hunter, K.A., and Kawahata, H., 2005, Global iron connections between desert dust, ocean biogeochemistry, and climate. *science*, 308 (5718), pp.67-71.
- Kamstra, J., 1987, *An Ecological Survey of the Cockscomb Basin, Belize*. Master's Thesis, York University, Ontario, Canada.

- Kesler, S.E., Kienle, C.F., and Bateson, J.H., 1974, Tectonic significance of the intrusive rocks in the Maya Mountains, British Honduras. *Geol. Soc. Am. Bull.* 85, pp. 549-552.
- Khalaf, F.I., and Gharib, I.M., 1985, Roundness parameters of quartz grains of recent aeolian sand deposits in Kuwait. *Sedimentary Geology*, 45(1-2), pp.147-158.
- King, R.B., Baillie, I.C., Dumsmore, J.R., Grimble, R.J., Johnson, M.S., Williams, J.B., and Wright, A.C.S., 1989, Land Resource Assessment of Stann Creek District, Belize. Chatham, UK: Overseas Development Natural Resource Institute.
- Knippertz, P., 2017, Mineral dust generation across northern Africa and its impacts. In *Oxford Research Encyclopedia of Climate Science*.
- Liu, X., Huneus, N., Schulz, M., Balkanski, Y., Griesfeller, J., Prospero, J., Kinne, S., Bauer, S., Boucher, O., Chin, M., and Dentener, F., 2011, Global dust model intercomparison in AeroCom phase I. *Atmospheric Chemistry and Physics*, 11(15), p.7781.
- Mahowald, N.M., Lindsay, K., Rothenberg, D., Doney, S.C., Moore, J.K., Thornton, P., Randerson, J.T., and Jones, C.D., 2011, Desert dust and anthropogenic aerosol interactions in the Community Climate System Model coupled-carbon-climate model. *Biogeosciences*, 8, 387–414.
- Martin, J.H., Gordon, M.R., and Fitzwater, S.E., 1991, The case for iron, *Limnology and Oceanography*. 36, doi: 10.4319/lo.1991.36.8.1793.

- Mazzullo, J.I.M., Sims, D., and Cunningham, D., 1986, The effects of eolian sorting and abrasion upon the shapes of fine quartz sand grains. *Journal of Sedimentary Research*, 56(1), pp.45-56.
- McBirney, A.R., and Bass, M.N., 1969, Structural relations of pre-Mesozoic rocks of northern Central America. *American Association of Petroleum Geologists Memoir* 11, p. 269-280.
- McCloskey, T.A., and Keller, G., 2009, 5000 year sedimentary record of hurricane strikes on the central coast of Belize. *Quaternary international*, 195(1-2), pp.53-68.
- Middleton, N.J., and Goudie, A.S., 2001, Saharan dust: sources and trajectories. *Transactions of the Institute of British Geographers*, 26 (2), pp.165-181.
- Muhs, D.R., 2013, The geologic records of dust in the Quaternary. *Aeolian Research*, 9, pp.3-48.
- Muhs, D.R., and Budahn, J.R., 2009, Geochemical evidence for African dust and volcanic ash inputs to terra rossa soils on carbonate reef terraces, northern Jamaica, West Indies. *Quaternary International*, 196(1-2), pp.13-35.
- Muhs, D.R., Budahn, J.R., Prospero, J.M., and Carey, S.N., 2007, Geochemical evidence for African dust inputs to soils of western Atlantic islands: Barbados, the Bahamas, and Florida. *Journal of Geophysical Research: Earth Surface*, 112 (F2).
- Muhs, D.R., Bush, C.A., Stewart, K.C., Rowland, T.R. and Crittenden, R.C., 1990, Geochemical evidence of Saharan dust parent material for soils developed on

- Quaternary limestones of Caribbean and western Atlantic islands. *Quaternary Research*, 33 (2), pp.157-177.
- Perry, K.D., Cahill, T.A., Eldred, R.A., Dutcher, D.D., and Gill, T.E., 1997, Long-range transport of North African Dust to the eastern United States. *J. Geophys. Res.*, 102, 11,225-11, 238.
- Petit, J.R., Mounier, L., Jouzel, J., Korotkevich, Y.S., Kotlyakov, V.I., and Lorius, C., 1990, Palaeoclimatological and chronological implications of the Vostok core dust record. *Nature*, 343, 56–58.
- Pielke Jr, R.A., Rubiera, J., Landsea, C., Fernández, M.L. and Klein, R., 2003, Hurricane vulnerability in Latin America and the Caribbean: Normalized damage and loss potentials. *Natural Hazards Review*, 4(3), pp.101-114.
- Prather, K.A., Hatch, C.D., and Grassian, V.H., 2008, Analysis of atmospheric aerosols. *Annual Review of Analytical Chemistry* 1:1, 485-514.
- Prospero, J.M., 1999, Long-term measurements of the transport of African mineral dust to the southeastern United States: Impact on regional air quality. *J. Geophys. Res.*, 104(D13), 15917–15927.
- Prospero, J.M., Blades, E., Mathison, G. and Naidu, R., 2005, Interhemispheric transport of viable fungi and bacteria from Africa to the Caribbean with soil dust. *Aerobiologia*, 21(1), pp.1-19.
- Prospero, J. M., and Carlson, T., 1972, Vertical and areal distribution of Saharan dust over the western equatorial North Atlantic Ocean. *J. Geophys. Res.*, 77, 5255–5265,

- Prospero, J.M., Collard, F.X., Molinié, J., and Jeannot, A., 2014, Characterizing the annual cycle of African dust transport to the Caribbean Basin and South America and its impact on the environment and air quality. *Global Biogeochemical Cycles*, 28(7), pp.757-773.
- Prospero, J.M., Ginoux, P., Torres, O., Nicholson, S.E. and Gill, T.E., 2002, Environmental characterization of global sources of atmospheric soil dust identified with the Nimbus 7 Total Ozone Mapping Spectrometer (TOMS) absorbing aerosol product. *Reviews of geophysics*, 40(1), pp.2-1.
- Prospero, J.M., Glaccum, R. a., and Nees, R.T., 1981, Atmospheric transport of soil dust from Africa to South America. *Nature* volume 289, pages 570–572.
- Prospero, J.M. and Mayol-Bracero, O.L., 2013, Understanding the transport and impact of African dust on the Caribbean basin. *Bulletin of the American Meteorological Society*, 94(9), pp.1329-1337.
- Qiang, M., Liu, Y., Jin, Y., Song, L., Huang, X., and Chen, F., 2014, Holocene record of eolian activity from Genggahai Lake, northeastern Qinghai-Tibetan Plateau, China, *Geophys. Res. Lett.*, 41, 589– 595, doi:10.1002/2013GL058806.
- Ramanathan, V., Crutzen, P.J., Kiehl, J.T., Rosenfeld, D., 2001, Aerosols, climate, and the hydrological cycle. *Science*, 294, 2119–2124
- Rea, D.K., 1994, The Paleoclimatic record provided by eolian deposition in the deep sea: The geologic history of wind. *Rev. Geophys.*, 32, 159–195.

- Reid, J.S., Westphal, D.L., Livingston, J.M., Savoie, D.L., Maring, H.B., Jonsson, H.H., Eleuterio, D.P., Kinney, J.E., and Reid, E.A., 2002, Dust vertical distribution in the Caribbean during the Puerto Rico Dust experiment. *Geophys. Res. Lett.*, 29(7), 1151, doi:10.1029/2001GL014092
- Schaetzle, R., Anderson, S., 2005, *Soils Genesis and Geomorphology*. Cambridge University Press
- Schepanski, K., Tegen, I., and Macke, A., 2009, Saharan dust transport and deposition towards the tropical northern Atlantic. *Atmos. Chem. Phys.*, 9, 1173–1189, doi:10.5194/acp-9-1173-2009
- Schoeneberger, P.J., Wasocki, D.A., Benham, E.C., and Soil Survey Staff, 2012, *Field book for describing and sampling soils. Version 3.0*, Natural Resource Conservation Service, National Soil Survey Center, Lincoln, NE.
- Shao, Y., Wyrwoll, K.H., Chappell, A., Huang, J., Lin, Z., McTainsh, G.H., Mikami, M., Tanaka, T.Y., Wang, X. and Yoon, S., 2011, Dust cycle: An emerging core theme in Earth system science. *Aeolian Research*, 2(4), pp.181-204.
- Singer, M.J., and Janitzky, P., 1986. *Field and laboratory procedures used in a soil chronosequence study (No. 1648)*. Department of the Interior, US Geological Survey.
- Smith, B.J., Wright, J.S. and Whalley, W.B., 2002, Sources of non-glacial, loess-size quartz silt and the origins of “desert loess”. *Earth-Science Reviews*, 59(1-4), pp.1-26.

- Steffensen, J.P., 1997, The size distribution of microparticles from selected segments of the Greenland Ice Core Project ice core representing different climatic periods. *J. Geophys. Res.*, 102 (C12), 26,755–26,763.
- Swap, R., Garstang, M., Greco, S., Talbot, and R., Kallberg, P., 1992, Saharan dust in the Amazon basin. *Tellus B*, 44: 133-149. doi:10.1034/j.1600-0889.1992.t01-1-00005.x
- Syers, J.K., Jackson, M.L., Berkheiser, V.E., Clayton, R.N. and Rex, R.W., 1969, Eolian sediment influence on pedogenesis during the Quaternary. *Soil Science*, 107(6), pp.421-427.
- Todd, M.C., Washington, R., Martins, J.V., Dubovik, O., Lizcano, G., M'Bainayel, S., and Engelstaedter, S., 2007, Mineral dust emission from the Bode'le' Depression, northern Chad, during BoDEx 2005. *J. Geophys. Res.*, 112, D062
doi:10.1029/2006JD007170
- Usher, C.R., Michel, A.E., Grassian, V.H., 2003, Reactions on mineral dust. *Chemical Reviews*, 103 (12), 4883-4940 DOI: 10.1021/cr020657y
- Walsh, C., Ward, L., O'Neill-Byrne, J., O'Neill-Byrne, K. and Herzberg, J.L., 1996, Belize: a new psychiatric service revisited. *Psychiatric Bulletin*, 20(4), pp.237-238.
- Weil, R.R., Brady, N.C., 2017, *The Nature and Properties of Soils*. 15th Edition., Global Edition, Person Education Limited
- Wright A.C.S., Romney D.H., Arbuckle R.H., and Vial V. E., 1959, *Land in British Honduras*. Colonial Research Publication, Her Majesty's Service Office, London, United Kingdom.

- Young, A., 1980, Tropical soils and soil survey. (Vol. 9). CUP Archive.
- Yu, H., Chin, M., Bian, H., Yuan, T., Prospero, J. M., Omar, A. H., Remer, L. A., Winker, D. M., Yang, Y., Zhang, Y., and Zhang, Z., 2015, Quantification of trans-Atlantic dust transport from seven-year (2007–2013) record of CALIPSO lidar measurements. *Remote Sensing of Environment* 159, 232–249.
- Zhang, D., Gao, X., Zaakey, A., and Giorgi F., 2016, Effects of climate changes on dust aerosol over East Asia from RegCM3. *Advances in Climate Change Research*, Vol. 7 pp. 145-153.
- Zhang, X., Tong, D.Q., Wu, G., Wang, X., Xiu, A., Han, Y., Xu, T., Zhang, S., and Zhao, H., 2016, Identification of dust sources and hotspots in East Asia during 2000–2015: implications for numerical modeling and forecasting. *Atmos. Chem. Phys. Discuss.*, <https://doi.org/10.5194/acp-2016-681>

APPENDIX A: WIND DIRECTION

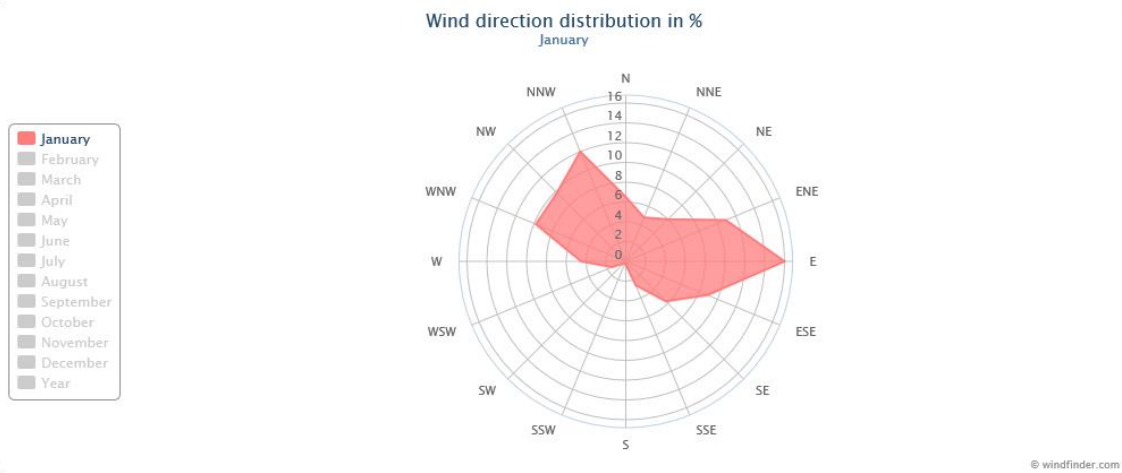


Figure A-1. Wind direction distribution in percentage graph indicating prevailing wind direction for the month of January, 2018. International Airport in Ladyville, Belize.

Windfinder.com

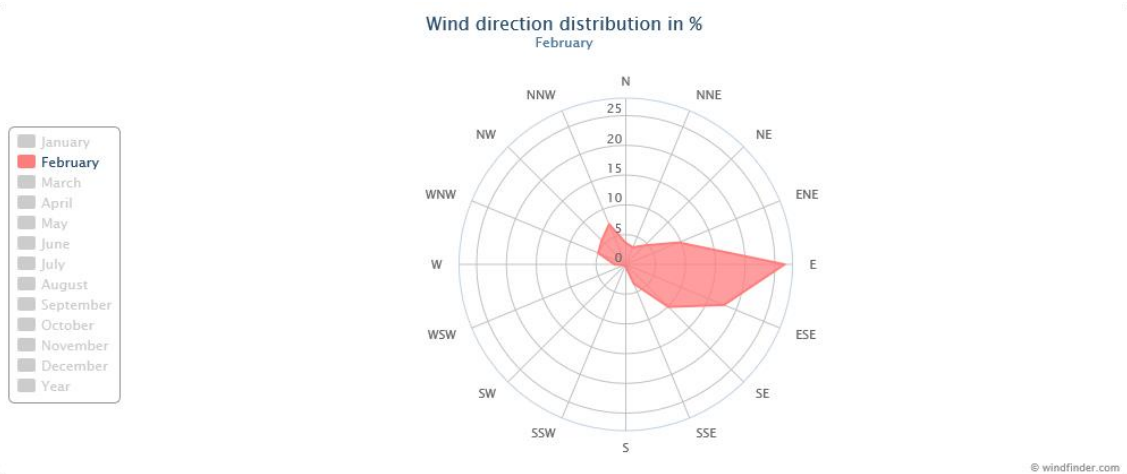


Figure A-2. Wind direction distribution in percentage graph indicating prevailing wind direction for the month of February, 2018. International Airport in Ladyville, Belize.

Windfinder.com

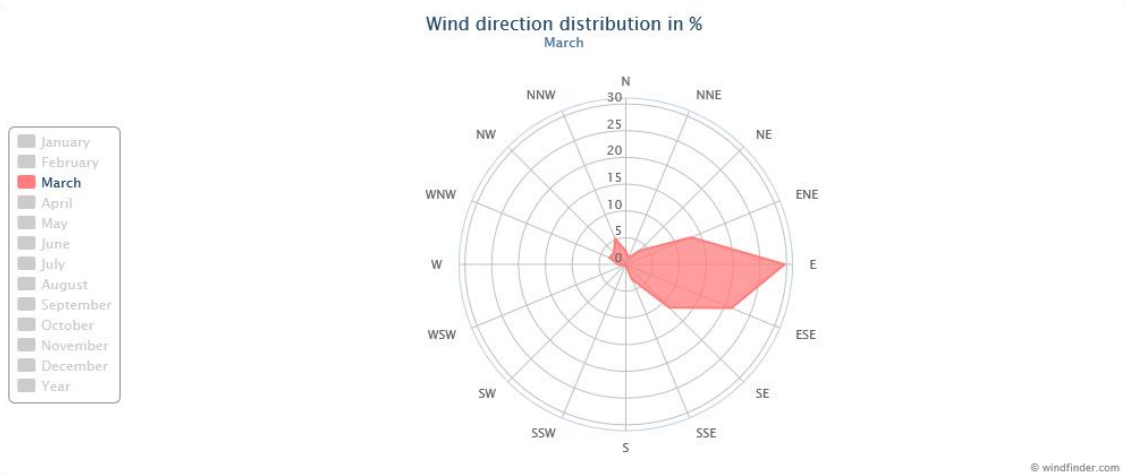


Figure A-3. Wind direction distribution in percentage graph indicating prevailing wind direction for the month of March, 2018. International Airport in Ladyville, Belize.

Windfinder.com

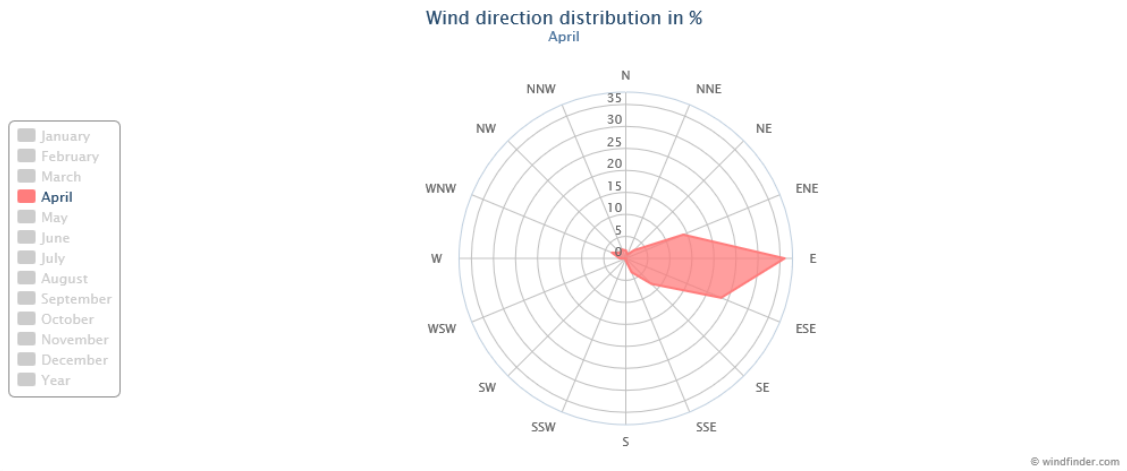


Figure A-4. Wind direction distribution in percentage graph indicating prevailing wind direction for the month of April, 2018. International Airport in Ladyville, Belize.

Windfinder.com

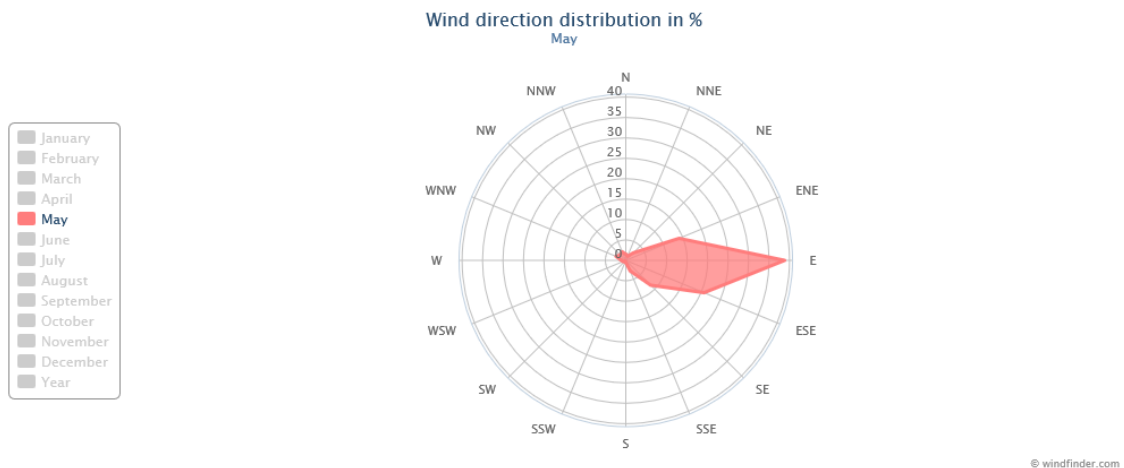


Figure A-5. Wind direction distribution in percentage graph indicating prevailing wind direction for the month of May, 2018. International Airport in Ladyville, Belize.

Windfinder.com

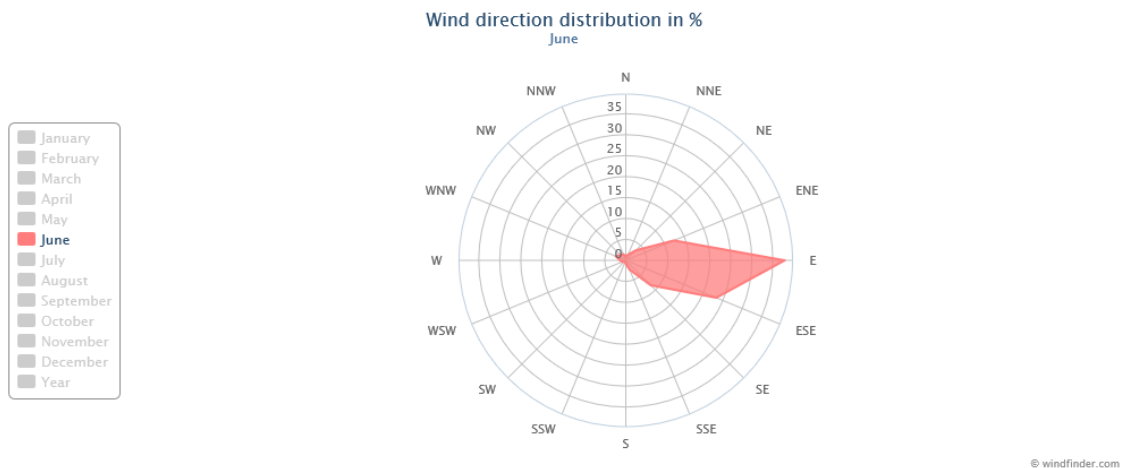


Figure A-6. Wind direction distribution in percentage graph indicating prevailing wind direction for the month of June, 2018. International Airport in Ladyville, Belize.

Windfinder.com

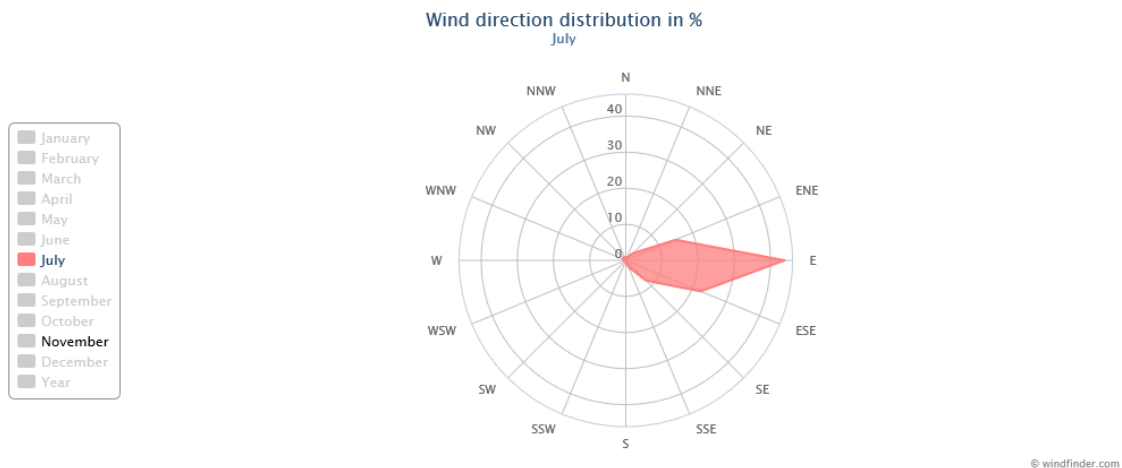


Figure A-7. Wind direction distribution in percentage graph indicating prevailing wind direction for the month of July, 2018. International Airport in Ladyville, Belize.

Windfinder.com

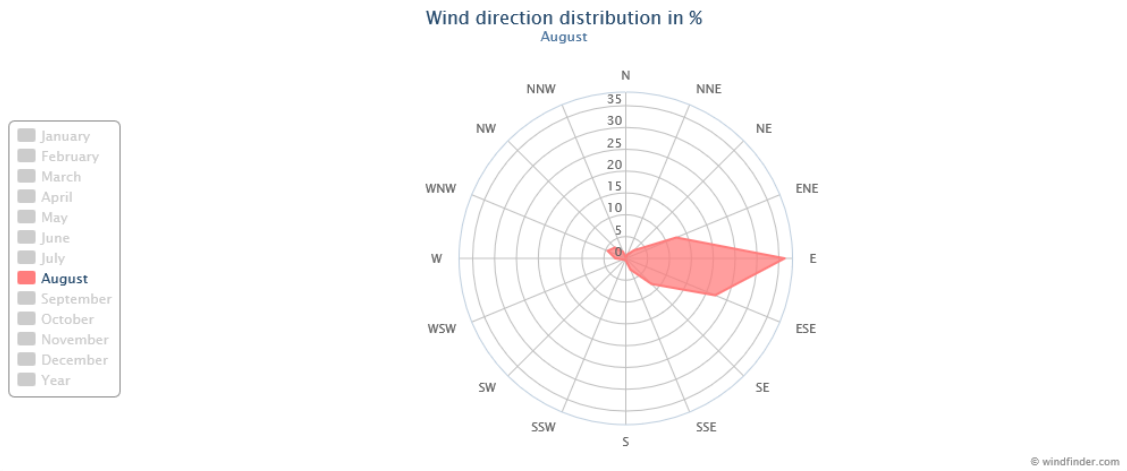


Figure A-8. Wind direction distribution in percentage graph indicating prevailing wind direction for the month of August, 2018. International Airport in Ladyville, Belize.

Windfinder.com

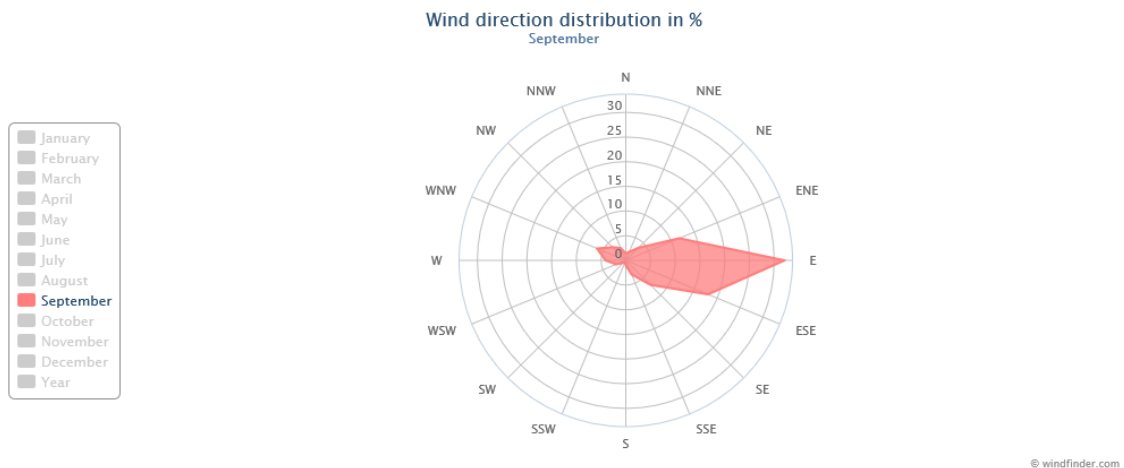


Figure A-9. Wind direction distribution in percentage graph indicating prevailing wind direction for the month of September, 2018. International Airport in Ladyville, Belize.

Windfinder.com

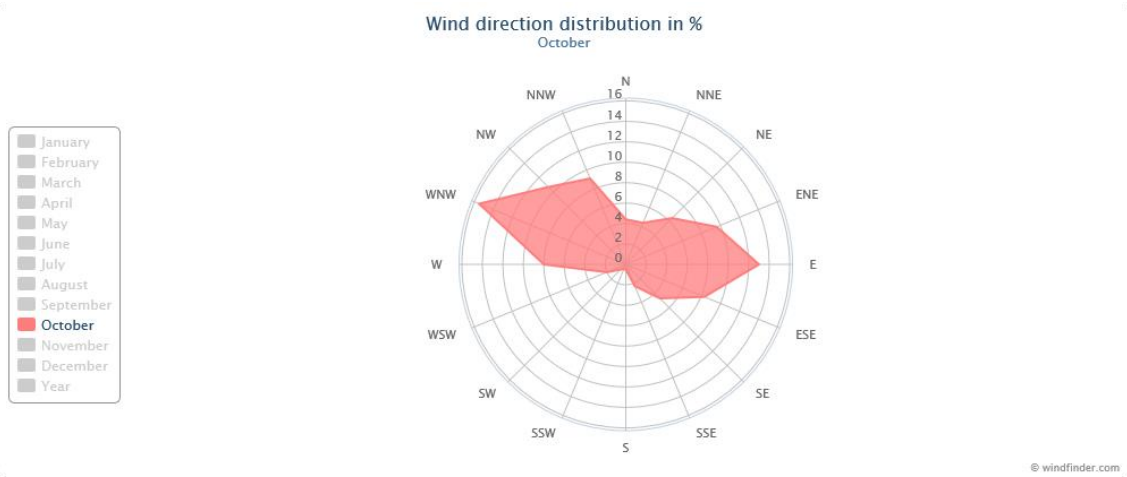


Figure A-10. Wind direction distribution in percentage graph indicating prevailing wind direction for the month of October, 2018. International Airport in Ladyville, Belize.

Windfinder.com

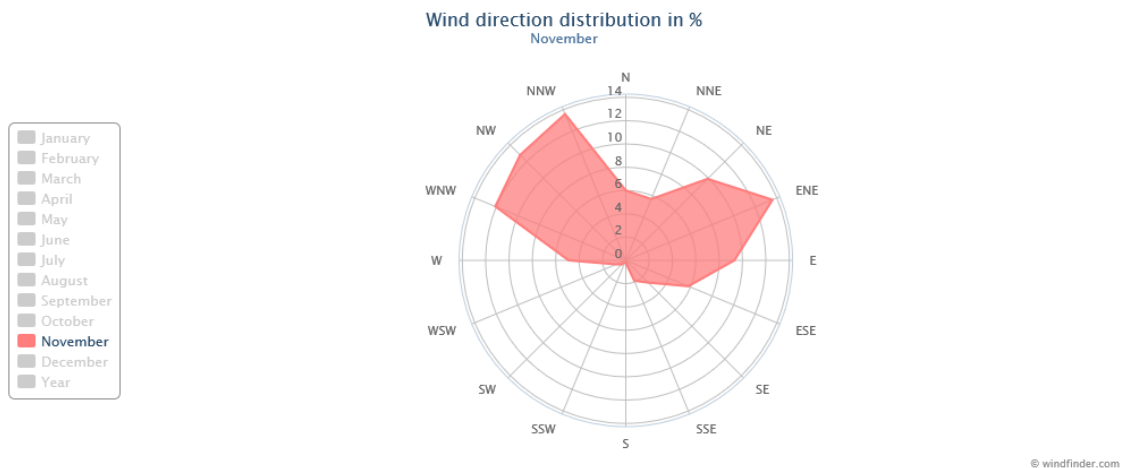


Figure A-11. Wind direction distribution in percentage graph indicating prevailing wind direction for the month of November, 2018. International Airport in Ladyville, Belize.

Windfinder.com

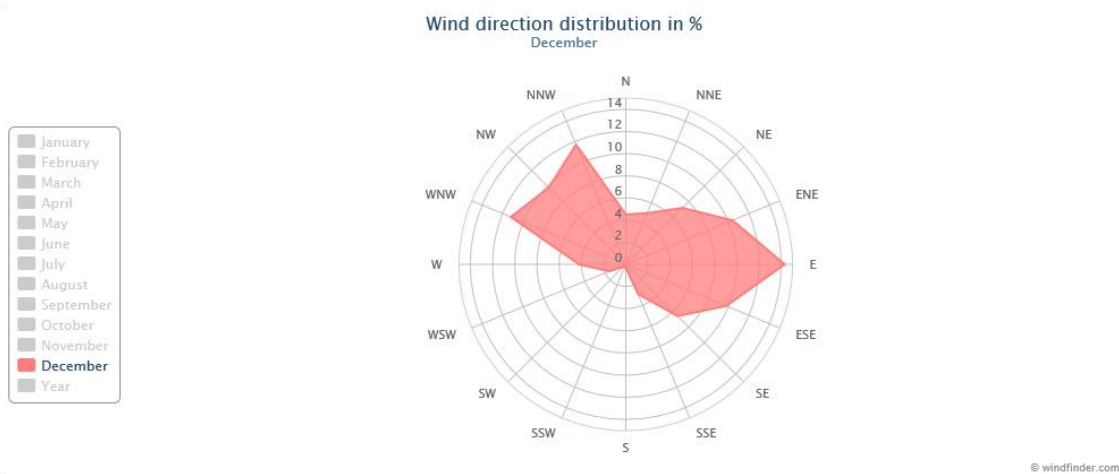


Figure A-12. Wind direction distribution in percentage graph indicating prevailing wind direction for the month of December, 2018. International Airport in Ladyville, Belize.

Windfinder.com

APPENDIX B: PARTICLE SIZE DISTRIBUTION ANALYSIS PROCEDURE

Procedure for pretreatment of particle size sub-sample and associated analyses.

Particle Size Distribution (PSD)

1.) Preparation

All samples were air dried, >2.00 mm (gravels) were separated from <2 mm (sands, silts, and clay) using a 2.00 mm sieve. Approximately 25 g representative sample of the <2 mm fraction was separated out, placed in a tared 600 ml beaker, adding enough distilled water to create a paste consistency with the sample. At this point, 5 ml of hydrogen peroxide was added to burn off organics, covered, and left minimum of 12 hours

2.) Dispersion

With a pipette, 25 ml of Sodium Hexametaphosphate was added to the sample, stirred, and left to sit for a minimum of 12 hours. The sample was then placed into an ultrasonic bath for 20 minutes and then wet sieved.

3.) Wet Sieve

Using distilled water, contents from the 600 ml beaker were washed through a 270-mesh screen sieve, into a clean bucket. Sand left in the 270-mesh sieve, was collected in a 250 ml tared beaker, and placed in a 110°C oven for a minimum of 12

hours. Once all water was cooked off, the beaker was transferred to a desiccator for 2-3 hours, and weight was recorded.

Stabilizing room temperature, silts and clays collected in the bucket were then poured into a 1000 ml graduated cylinder, using enough distilled water to clean out all residual silts and clays, and to reach the 1000 ml meniscus line.

Using a metal plunger, contents of the graduated cylinder were well mixed. After mixing, a 25 ml pipette was inserted to a depth of 20 cm, after waiting 20 seconds, a draw was taken for silt and clay. Contents of the pipette were then placed into a tared 100 ml beaker, and placed into a 110°C oven for a minimum of 12 hours to dry. The 100 ml beaker was then transferred to a desiccator for 2-3 hours to cool, and weighed to determine the silt, clay fraction.

The silt was then allowed to settle (3-4 hours), at which time, a 25 ml pipette was inserted to a depth of 5 cm into the remaining sample of the graduated cylinder, and a clay draw was taken. Contents of the pipette were then transferred into a tared 50 ml beaker, and placed into a 110°C oven for a minimum of 12 hours to dry. The beaker was then transferred to a desiccator for 2-3 hours to cool, then weighed for the clay fraction.

APPENDIX C: SOIL DESCRIPTIONS AND LABORATORY DATA

Cockscomb Basin Wildlife Sanctuary: Map Area 1; Catena Transect, Pedon 1

Location^a	Cockscomb Basin Wildlife Sanctuary, East Basin	Surficial map unit	Q1	Date	3/22/2013
Soil Profile	Pedon 1	Geomorphic Surface	Basin	Time	0900 hrs
UTM^b	1857856mN 0341668mE	Surface altitude^c	127 m 416.6 ft	Described by	Heath Sawyer
Slope	<33° South East	Parent Materials	Sapote Granite	Notes by	Mitch Danforth
Aspect	South East	Vegetation	Broad-Leaved Forest		

Field Description^d

Horizon	Depth, cm	Color		Structure	Gravel, % (visual)	Consistence			Clay Films	Lower Boundary	Texture (field)	Field estimate			pH (field)	CaCO ₃ (field)	
		moist	dry			wet	moist	dry				sand	silt	clay		stage	effervescence
A	0-9	10YR 2/2	10YR 4/2	3sbk-vf-f	4	-	fr	mh	-	c, s	1	-	-	21	7	nil	NE
A2	09-50	10YR 2/2	10YR 5/3	2sbk-vf-m	10	-	vfr	sh	-	d, w	1	-	-	20	7	nil	NE
Bt	50-82	10YR 4/3	10YR 5/4	2sbk-vf-m	15	-	vfr	sh	D, D, B; T, f, I	g, i	1	-	-	16	7	nil	NE
C	82-100	10YR 5/4	10YR 7/4	1sbk-m-co	23	-	fr	sh	T, D, I, D, D, B		sl	-	-	18	7	nil	NE

^a Plate 1; ^b UTM coordinates: WGS84, Zone 16Q; ^c Data obtained using a hand held Garmin GPSmap 62s; ^d USDA Soil Survey nomenclature (2012) NA = Not Applicable; dashes

Location^a	Cockscomb Basin Wildlife Sanctuary, East Basin	Surficial map unit	Q1	Date	3/22/2013
Soil Profile	Pedon 1	Geomorphic Surface	Basin	Time	0900 hrs
UTM^b	1857856mN 0341668mE	Surface altitude^c	127 m 416.6 ft	Described by	Heath Sawyer
Slope	<33° South East	Parent Materials	Sapote Granite	Notes by	Mitch Danforth
Aspect	South East	Vegetation	Broad-Leaved Forest		

Field Description and Lab Data^d

Horizon	Depth, cm	Color		Structure	Gravel, % (visual)	Consistence			Clay Films	Lower Boundary	Texture (lab)	Grain size, wt %			pH (field)	CaCO ₃ (field)	
		moist	dry			wet	moist	dry				sand	silt	clay		stage	effervescence
A	0-9	10YR 2/1	10YR 4/2	3sbk-vf-f	4	-	fr	mh	-	c, s	1	52	32	16	7	nil	NE
A2	09-50	10YR 2/1	10YR 5/3	2sbk-vf-m	10	-	vfr	sh	-	d, w	1	59	29	12	7	nil	NE
Bt	50-82	10YR 4/3	10YR 5/4	2sbk-vf-m	15	-	vfr	sh	D, D, B; T, f, I	g, i	1	49	34	18	7	nil	NE
CB	82-100	10YR 5/4	10YR 7/4	1sbk-m-co	23	-	fr	sh	T, D, I, D, D, B	-	sl	52	34	14	7	nil	NE

Figure C-1. Field and Laboratory pedon descriptions, Pedon 1, top of catena transect (summit).

Cockscomb Basin Wildlife Sanctuary: Map Area 1; Catena Transect, Pedon 2

Location^a	Cockscomb Basin Wildlife Sanctuary, East Basin	Surficial map unit	Ql	Date	3/18/2013
Soil Profile	Pedon 2	Geomorphic Surface	Basin	Time	1310 hrs
UTM^b	1857676mN 0341670mE	Surface altitude^c	104 m 341.2 ft	Described by	Heath Sawyer
Slope	<45° South East	Parent Materials	Sapote Granite	Notes by	Mitch Danforth
Aspect	South East	Vegetation	Broad -Leaved Forest		

Field Description^d

Horizon	Depth, cm	Color		Structure	Gravel, % (visual)	Consistence			Clay Films	Lower Boundary	Texture (field)	Field estimate			pH (field)	CaCO ₃ (field)	
		moist	dry			wet	moist	dry				sand	silt	clay		stage	effervescence
A	0-24	10YR 2/2	10YR 5/3	2sbk-f	45	-	vfr	sh	-	g, s	l	-	-	18	5	nil	NE
AC	24-35	10YR 2/2	10YR 5/3	1sbk-f	55	-	vfr	sh	-	c, s	sl	-	-	20	6	nil	NE
C	35-60	2.5YR 4/8	5YR 7/6	1sbk-f	40	-	vfr	sh	-	-	scl	-	-	22	6	nil	NE

^a Plate 1; ^b UTM coordinates: WGS84, Zone 16Q; ^c Data obtained using a hand held Garmin GPSmap 62s; ^d USDA Soil Survey nomenclature (2012) NA = Not Applicable; dashes

Location^a	Cockscomb Basin Wildlife Sanctuary, East Basin	Surficial map unit	Ql	Date	3/18/2013
Soil Profile	Pedon 2	Geomorphic Surface	Basin	Time	1310 hrs
UTM^b	1857676mN 0341670mE	Surface altitude^c	104 m 341.2 ft	Described by	Heath Sawyer
Slope	<45° South East	Parent Materials	Sapote Granite	Notes by	Mitch Danforth
Aspect	South East	Vegetation	Broad -Leaved Forest		

Field Description and Lab Data^d

Horizon	Depth, cm	Color		Structure	Gravel, % (visual)	Consistence			Clay Films	Lower Boundary	Texture (lab)	Grain size, wt %			pH (field)	CaCO ₃ (field)	
		moist	dry			wet	moist	dry				sand	silt	clay		stage	effervescence
A	0-24	10YR 2/2	10YR 5/3	2sbk-f	45	-	vfr	sh	-	g, s	sl	64	18	18	5	nil	NE
AC	24-35	10YR 2/2	10YR 5/3	1sbk-f	55	-	vfr	sh	-	c, s	sl	67	17	16	6	nil	NE
C	35-60	2.5YR 4/8	5YR 7/6	1sbk-f	40	-	vfr	sh	-	-	sl	69	15	16	6	nil	NE

Figure C-2. Field and Laboratory pedon descriptions, Pedon 2, catena transect; shoulder slope position.

Cockscomb Basin Wildlife Sanctuary: Map Area 1; Catena Transect, Pedon 3

Location^a	Cockscomb Basin Wildlife Sanctuary, East Basin	Surficial map unit	Ql	Date	3/18/2013
Soil Profile	Pedon 3	Geomorphic Surface	Basin	Time	0910 hrs
UTM^b	1857447mN 0341694mE	Surface altitude^c	94 m 308.4 ft	Described by	Heath Sawyer
Slope	<2° South East	Parent Materials	Sapote Granite	Notes by	Mitch Danforth
Aspect	South East	Vegetation	Broad-Leaved Forest		

Field Description^d

Horizon	Depth, cm	Color		Structure	Gravel, % (visual)	Consistence			Clay Films	Lower Boundary	Texture (field)	Field estimate			pH (field)	CaCO ₃ (field)	
		moist	dry			wet	moist	dry				sand	silt	clay		stage	effervescence
A	0-22	10YR 2/1	10YR 4/2	2gr-f	1	-	fr	mh	T, f, I	g, w	sil	-	-	18	5	nil	NE
A2	22-43	10YR 2/1	10YR 5/2	2gr-f	2	-	fr	sh	-	d, s	l	-	-	20	5	nil	NE
A3	43-86	10YR 4/3	10YR 7/3	1sbk-f	5	-	fr	mh	D, f, B	g, s	scl	-	-	23	5	nil	NE
C	86-100	10YR 5/4	2.5Y 7/4	m	15	-	fr	mh	T, f, I; D, f, R	-	cl	-	-	33	5	nil	NE

^a Plate 1; ^b UTM coordinates: WGS84, Zone 16Q; ^c Data obtained using a hand held Garmin GPSmap 62s; ^d USDA Soil Survey nomenclature (2012) NA = Not Applicable; dashes

Location^a	Cockscomb Basin Wildlife Sanctuary, East Basin	Surficial map unit	Ql	Date	3/18/2013
Soil Profile	Pedon 3	Geomorphic Surface	Basin	Time	0910 hrs
UTM^b	1857447mN 0341694mE	Surface altitude^c	94 m 308 ft	Described by	Heath Sawyer
Slope	<2° South East	Parent Materials	Sapote Granite	Notes by	Mitch Danforth
Aspect	South East	Vegetation	Broad-Leaved Forest		

Field Description and Lab Data^d

Horizon	Depth, cm	Color		Structure	Gravel, % (visual)	Consistence			Clay Films	Lower Boundary	Texture (lab)	Grain size, wt %			pH (field)	CaCO ₃ (field)	
		moist	dry			wet	moist	dry				sand	silt	clay		stage	effervescence
A	0-22	10YR 2/1	10YR 6/2	2gr-f	1	-	fr	mh	T, f, I	g, w	l	51	29	20	5	nil	NE
AB	22-43	10YR 2/1	10YR 6/2	2gr-f	2	-	fr	sh	-	d, s	l	58	25	17	5	nil	NE
BA	43-86	10YR 4/3	10YR 6/2	1sbk-f	5	-	fr	mh	D, f, B	g, s	l	60	20	20	5	nil	NE
Bt	86-100	10YR 5/4	2.5Y 7/4	m	15	-	fr	mh	T, f, I; D, f, R	-	c	39	14	46	5	nil	NE

Figure C-3. Field and Laboratory pedon descriptions, Pedon 2, catena transect; backslope position.

Cockscomb Basin Wildlife Sanctuary: Map Area 1; Catena Transect, Pedon 4

Location^a	Cockscomb Basin Wildlife Sanctuary, East Basin	Surficial map unit	Q1	Date	3/17/2013
Soil Profile	Pedon 4	Geomorphic Surface	Basin	Time	1240 hrs
UTM^b	1857364mN 0341684mE	Surface altitude^c	89 m 292 ft	Described by	Heath Sawyer
Slope	<10° South East	Parent Materials	Sapote Granite	Notes by	Mitch Danforth
Aspect	South East	Vegetation	Broad -Leaved Forest		

Field Description^d

Horizon	Depth, cm	Color		Structure	Gravel, % (visual)	Consistence		Clay Films	Lower Boundary	Texture (field)	Field estimate			pH (field)	CaCO ₃ (field)		
		moist	dry			wet	moist				dry	sand	silt		clay	stage	effervescence
A	0-6	10YR 4/2	10YR 6/2	3sbk-f	-	-	fr	mh	-	c, s	1	-	-	27	5	nil	NE
A2	6-30	10YR 4/2	10YR 6/2	2sbk-f	-	-	fr	mh	-	g, s	1	-	-	25	5	nil	NE
BA	30-39	10YR 4/2	10YR 6/2	1abk-m	-	-	fr	sh	T, f, I	c, w	1	-	-	25	5	nil	NE
B	39-100	5YR 5/8	7.5YR 7/8	1abk-co	-	-	fi	vh	T, f, I	cl	-	-	-	30	5	nil	NE

^a Plate 1; ^b UTM coordinates: WGS84, Zone 16Q; ^c Data obtained using a hand held Garmin GPSmap 62s; ^d USDA Soil Survey nomenclature (2012) NA = Not Applicable; dashes

Location^a	Cockscomb Basin Wildlife Sanctuary, East Basin	Surficial map unit	Q1	Date	3/17/2013
Soil Profile	Pedon 4	Geomorphic Surface	Basin	Time	1240 hrs
UTM^b	1857364mN 0341684mE	Surface altitude^c	89 m 292 ft	Described by	Heath Sawyer
Slope	<10° South East	Parent Materials	Sapote Granite	Notes by	Mitch Danforth
Aspect	South East	Vegetation	Broad -Leaved Forest		

Field Description and Lab Data^d

Horizon	Depth, cm	Color		Structure	Gravel, % (visual)	Consistence		Clay Films	Lower Boundary	Texture (lab)	Grain size, wt %			pH (field)	CaCO ₃ (field)		
		moist	dry			wet	moist				dry	sand	silt		clay	stage	effervescence
A	0-6	10YR 4/2	10YR 6/2	3sbk-f	-	-	fr	mh	-	c, s	sicl	38	31	31	5	nil	NE
A2	6-30	10YR 4/2	10YR 6/2	2sbk-f	-	-	fr	mh	-	g, s	1	45	27	28	5	nil	NE
BA	30-39	10YR 4/2	10YR 6/2	1sbk-m	-	-	fr	sh	T, f, I	c, w	1	43	25	32	5	nil	NE
Bt	39-100	5YR 5/8	7.5 Y/8	1sbk-co	-	-	fi	vh	T, f, I	cl	-	30	30	39	5	nil	NE

Figure C-4. Field and Laboratory pedon descriptions, Pedon 4, catena transect; footslope position.

Cockscomb Basin Wildlife Sanctuary: Map Area 1; Catena Transect, Pedon 5

Location^a	Cockscomb Basin Wildlife Sanctuary, East Basin	Surficial map unit	Q1	Date	3/17/2013
Soil Profile	Pedon 5	Geomorphic Surface	Basin	Time	0845 hrs
UTM^b	1857301mN 0341728mE	Surface altitude^c	80 m 262.5 ft	Described by	Heath Sawyer
Slope	<2° South East	Parent Materials	Sapote Granite	Notes by	Mitch Danforth
Aspect	South East	Vegetation	Broad -Leaved Forest		

Field Description^d

Horizon	Depth, cm	Color		Structure	Gravel, % (visual)	Consistence			Clay Films	Lower Boundary	Texture (field)	Field estimate			pH (field)	CaCO ₃ (field)	
		moist	dry			wet	moist	dry				sand	silt	clay		stage	effervescence
A	0-9	10YR 3/3	10YR 6/3	3sbk-f	2	-	fi	mh	-	a,w	l	-	-	24	5	nil	NE
Brw	9-20	10YR 4/4	10YR 6/4	3sbk-f	45	-	fr	sh	D, f, B	g,w	scl	-	-	22	6	nil	NE
B	20-29	10YR 4/3	10YR 6/3	2sbk-f	35	-	fr	sh	D, f, B; T, f, I	c,w	scl	-	-	20	6	nil	NE
C	29-41	5YR 5/8	7.5YR 7/6	1sbk-co	64	-	fr	sh	D, f, B	-	scl	-	-	26	6	nil	NE

^a Plate 1; ^b UTM coordinates: WGS84, Zone 16Q; ^c Data obtained using a hand held Garmin GPSmap 62s; ^d USDA Soil Survey nomenclature (2012) NA = Not Applicable; dashes

Location^a	Cockscomb Basin Wildlife Sanctuary, East Basin	Surficial map unit	Q1	Date	3/17/2013
Soil Profile	Pedon 5	Geomorphic Surface	Basin	Time	0845 hrs
UTM^b	1857301mN 0341728mE	Surface altitude^c	80 m 262.5 ft	Described by	Heath Sawyer
Slope	<2° South East	Parent Materials	Sapote Granite	Notes by	Mitch Danforth
Aspect	South East	Vegetation	Broad -Leaved Forest		

Field Description and Lab Data^d

Horizon	Depth, cm	Color		Structure	Gravel, % (visual)	Consistence			Clay Films	Lower Boundary	Texture (lab)	Grain size, wt %			pH (field)	CaCO ₃ (field)	
		moist	dry			wet	moist	dry				sand	silt	clay		stage	effervescence
A	0-9	10YR 3/3	10YR 6/3	3sbk-f	2	-	fr	mh	-	a,w	l	55	21	24	5	nil	NE
A2	9-20	10YR 4/4	10YR 6/4	3sbk-f	45	-	fr	sh	-	g,w	sl	66	16	18	6	nil	NE
AC	20-29	10YR 4/3	10YR 6/3	2sbk-f	35	-	fi	sh	-	c,w	scl	65	12	23	6	nil	NE
C	29-41	5YR 5/8	7.5 Y/6	1sbk-co	64	-	vfi	sh	-	-	cl	51	11	38	6	nil	NE

Figure C-5. Field and Laboratory pedon descriptions, Pedon 4, catena transect; toeslope position.

Cockscomb Basin Wildlife Sanctuary: Map Area 1; Catena Transect, Pedon 6

Location^a	Cockscomb Basin Wildlife Sanctuary, East Basin	Surficial map unit	Q1	Date	4/15/2013
Soil Profile	Pedon 6	Geomorphic Surface	Basin	Time	0845 hrs
UTM^b	1856050mN 0341948mE	Surface altitude^c	69 m 226.4 ft	Described by	Heath Sawyer
Slope	<2° East	Parent Materials	Sapote Granite	Notes by	Mitch Danforth
Aspect	East	Vegetation	Broad -Leaved Forest		

Field Description^d

Horizon	Depth, cm	Color		Structure	Gravel, % (visual)	Consistence		Clay Films	Lower Boundary	Texture (field)	Field estimate			pH (field)	CaCO ₃ (field)		
		moist	dry			wet	moist				dry	sand	silt		clay	stage	effervescence
A	0-11	10YR 4/4	10YR 6/3	3sbk-vf-co	-	-	fr	sh	-	c, s	1	-	-	16	6	mil	NE
A2	11-62	10YR 5/6	10YR 7/4	1abk-f-co	-	-	fr	sh	-	g, c	1	-	-	16	6	mil	NE
C	62-100	10YR 4/6	5YR 6/4	1abk-f-vc	1	-	vfr	sh	-	sl	-	-	-	10	6	mil	NE

^a Plate 1; ^b UTM coordinates: WGS84, Zone 16Q; ^c Data obtained using a hand held Garmin GPSmap 62s; ^d USDA Soil Survey nomenclature (2012) NA = Not Applicable; dashes

Location^a	Cockscomb Basin Wildlife Sanctuary, East Basin	Surficial map unit	Q1	Date	4/15/2013
Soil Profile	Pedon 6	Geomorphic Surface	Basin	Time	0845 hrs
UTM^b	1856050mN 0341948mE	Surface altitude^c	69 m 226.4 ft	Described by	Heath Sawyer
Slope	<2° East	Parent Materials	Sapote Granite	Notes by	Mitch Danforth
Aspect	East	Vegetation	Broad -Leaved Forest		

Field Description and Lab Data^d

Horizon	Depth, cm	Color		Structure	Gravel, % (visual)	Consistence		Clay Films	Lower Boundary	Texture (lab)	Grain size, wt %			pH (field)	CaCO ₃ (field)		
		moist	dry			wet	moist				dry	sand	silt		clay	stage	effervescence
A	0-11	10YR 4/4	10YR 6/3	3sbk-vf-co	-	-	fr	sh	-	c, s	1	41	35	25	6	mil	NE
A2	11-62	10YR 5/6	10YR 7/4	1abk-f-co	-	-	fr	sh	-	g, c	1	41	33	26	6	mil	NE
C	62-100	10YR 4/6	5YR 6/4	1abk-f-vc	1	-	vfr	sh	-	1	1	41	33	26	6	mil	NE

Figure C-6. Field and Laboratory pedon descriptions, Pedon 6, floodplain – 1.

Cockscomb Basin Wildlife Sanctuary: Map Area 1; Catena Transect, Pedon 7

Location^a	Cockscomb Basin Wildlife Sanctuary, East Basin		Surficial map unit	Q1	Date	5/18/2013
Soil Profile	Pedon 7		Geomorphic Surface	Basin	Time	1330 hrs
UTM^b	1855165mN	0341771mE	Surface altitude^c	78 m 260 ft	Described by Heath Sawyer	
Slope	<2° South East		Parent Materials	Sapote Granite	Notes by Mitch Danforth	
Aspect	South East		Vegetation	Broad-Leaved Forest		

Field Description^d

Horizon	Depth, cm	Color		Structure	Gravel, % (visual)	Consistence			Clay Films	Lower Boundary	Texture (field)	Field estimate			pH (field)	CaCO ₃ (field)	
		moist	dry			wet	moist	dry				sand	silt	clay		stage	effervescence
A	0-13	10YR 4/3	10YR 5/3	3sbk-vf-co	1	-	fr	sh	-	c, s	1	-	-	12	6	nil	NE
Bt	13-47	10YR 4/4	10YR 5/6	2sbk-f-co	-	-	fi	sh	T, f, P	d, s	1	-	-	15	6	nil	NE
Bc	47-100	10YR 4/4	5YR 5/6	1abk-m-vc	>1	-	vfr	sh	Z, f, B	-	sl	-	-	8	6	nil	NE

^a Plate 1; ^b UTM coordinates: WGS84, Zone 16Q; ^c Data obtained using a hand held Garmin GPSmap 62s; ^d USDA Soil Survey nomenclature (2012) NA = Not Applicable; dashe

Location^a	Cockscomb Basin Wildlife Sanctuary, East Basin		Surficial map unit	Q1	Date	3/18/2013
Soil Profile	Pedon 7		Geomorphic Surface	Basin	Time	1310 hrs
UTM^b	1855165mN	0341771mE	Surface altitude^c	78 m 260 ft	Described by Heath Sawyer	
Slope	<2° South East		Parent Materials	Sapote Granite	Notes by Mitch Danforth	
Aspect	South East		Vegetation	Broad-Leaved Forest		

Field Description and Lab Data^d

Horizon	Depth, cm	Color		Structure	Gravel, % (visual)	Consistence			Clay Films	Lower Boundary	Texture (lab)	Grain size, wt %			pH (field)	CaCO ₃ (field)	
		moist	dry			wet	moist	dry				sand	silt	clay		stage	effervescence
A	0-13	10YR 4/4	10YR 6/3	3sbk-vf-co	-	-	fr	sh	-	c, s	sl	54	32	13	6	nil	NE
Bt	13-47	10YR 5/6	10YR 7/4	1abk-f-co	-	-	fr	sh	T, f, P	g, c	1	24	48	27	6	nil	NE
CB	47-100	10YR 4/6	5YR 6/4	1abk-f-vc	1	-	vfr	sh	Z, f, B	-	sl	58	29	14	6	nil	NE

Figure C-7. Field and Laboratory pedon descriptions, Pedon 7, floodplain – 2.

APPENDIX D: PEDON PROFILE PARTICLE SIZE DISTRIBUTION

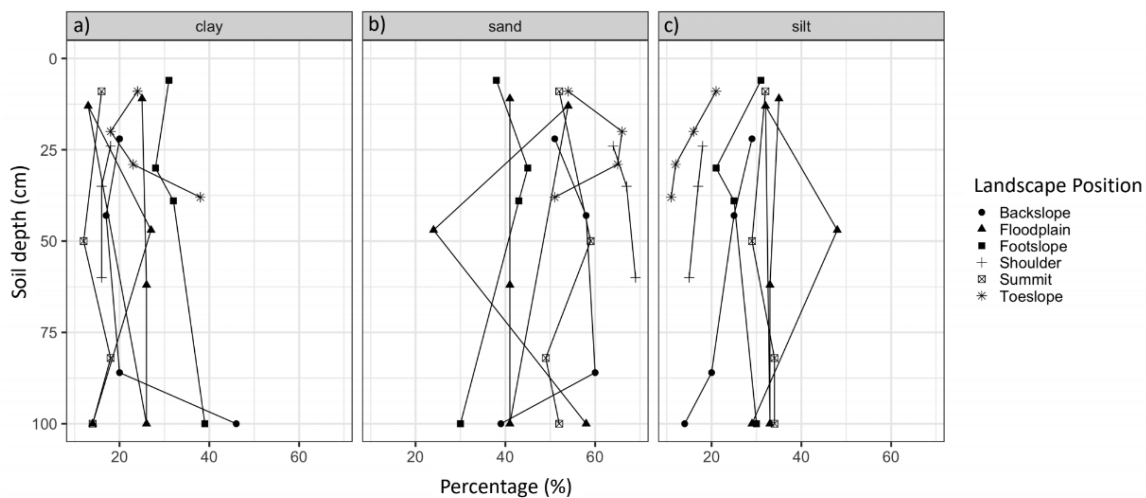


Figure D-1. Laboratory particle size distribution plots of clay, sand, and silt percentages, catena landscape position (illustrated by symbols) and horizon depth (cm).

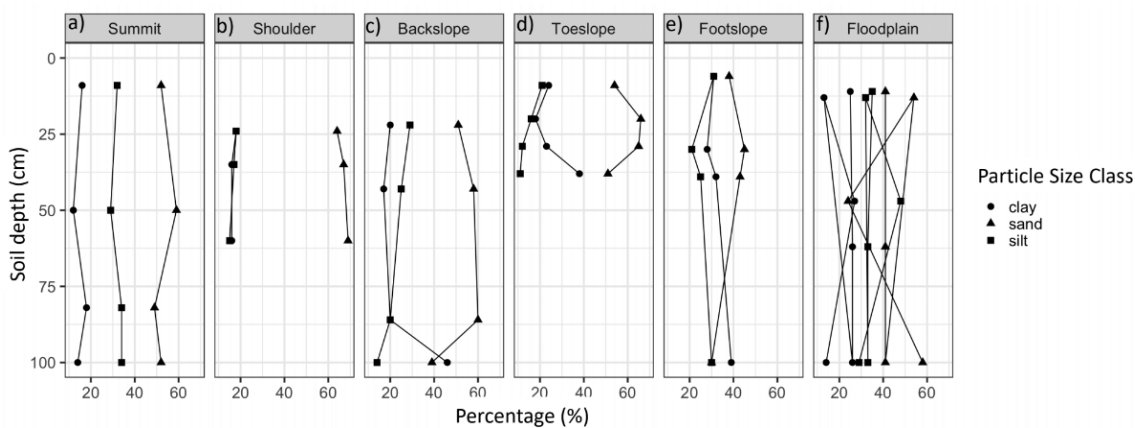


Figure D-2. Laboratory particle size distribution plots of clay, sand, and silt percentages along individual catena landscape positions (illustrated in symbols) and horizon depth (cm).

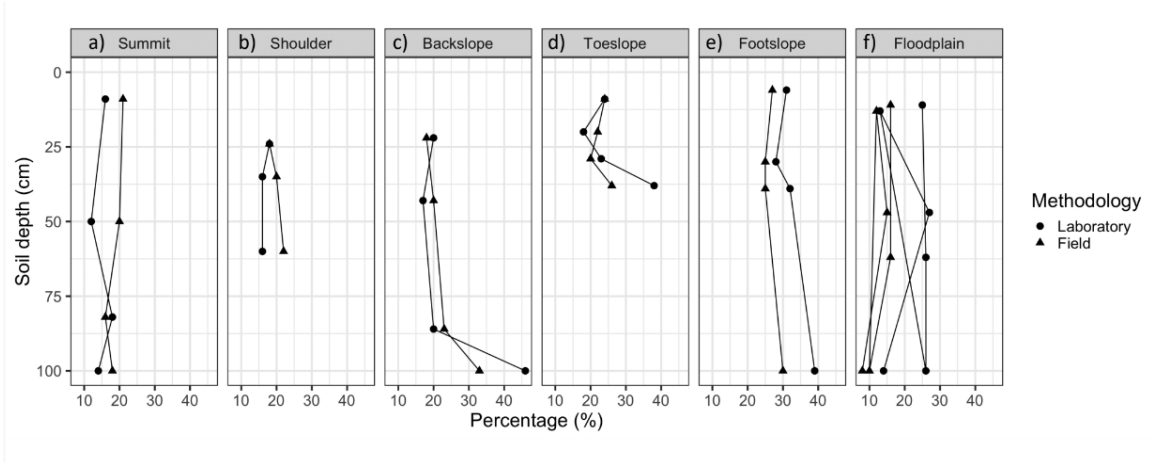


Figure D-3. Plots of catena transect slope position, illustrating pedon horizon depth (cm) and field clay percentage estimates plotted along side laboratory clay percentage measurements (illustrated by symbols).

APPENDIX E: X-RAY DIFFRACTION ANALYSIS GRAPHS

Pedon 1

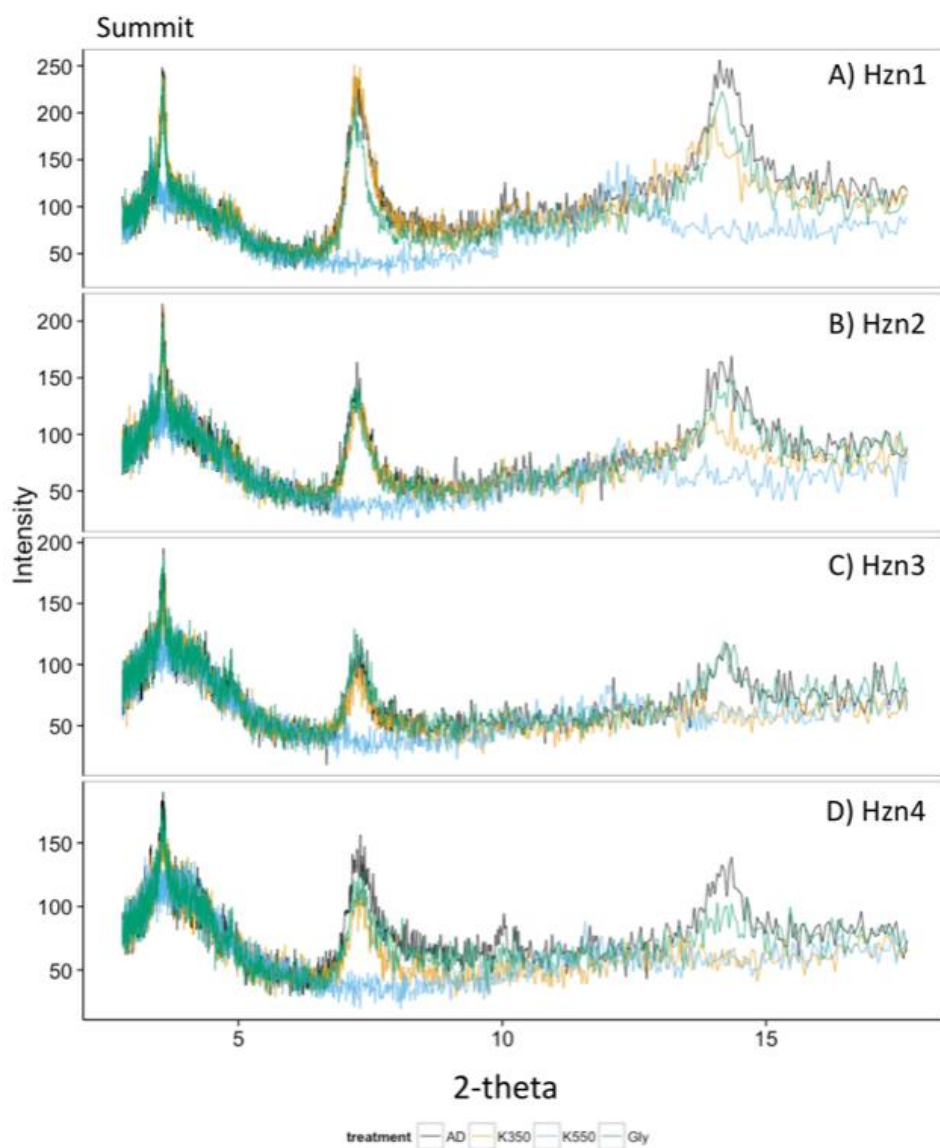


Figure E-1. X-ray diffraction diffractograms of each horizon of Pedon 1 (summit), representing primary clay mineralogy of kaolinite.

Pedon 2

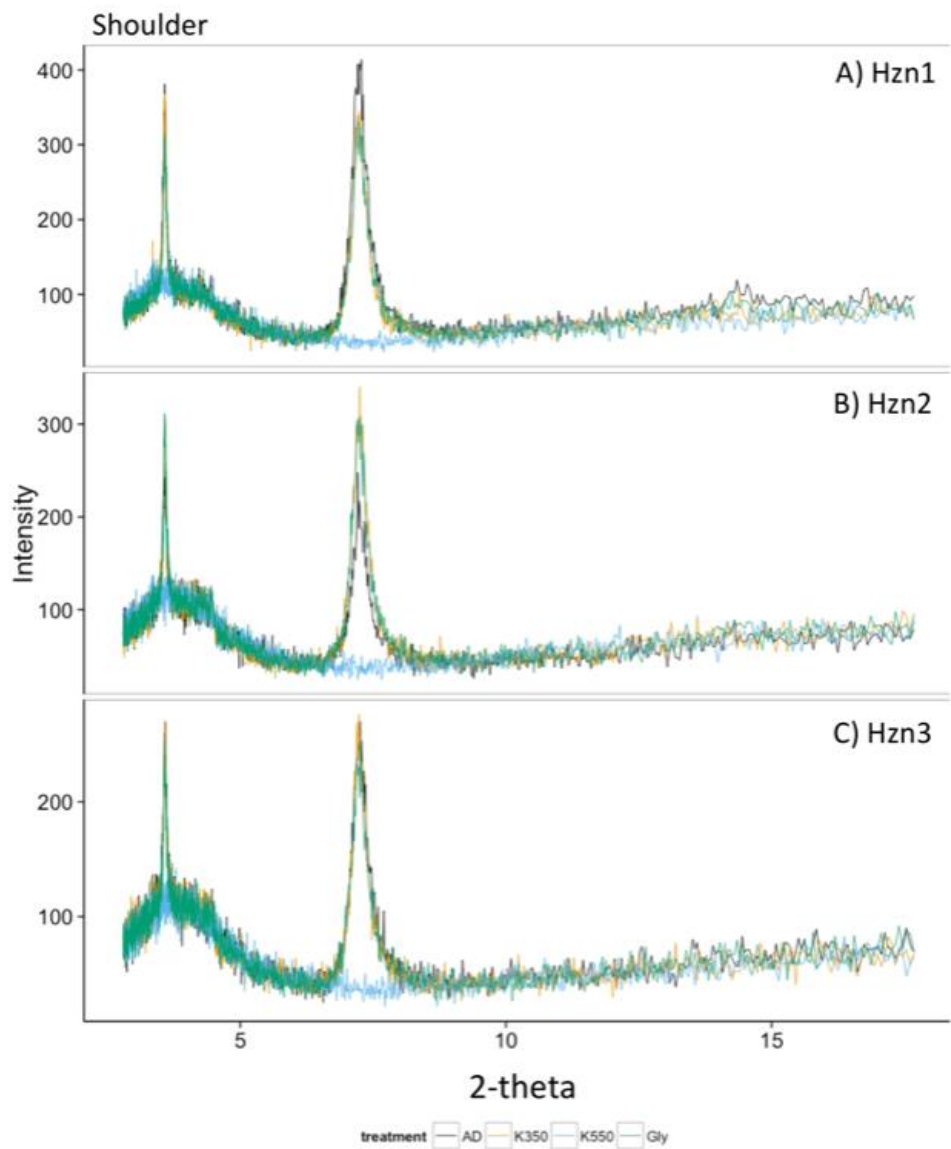


Figure E-2. X-ray diffraction diffractograms of each horizon of Pedon 2 (shoulder), representing primary clay mineralogy of kaolinite.

Pedon 3

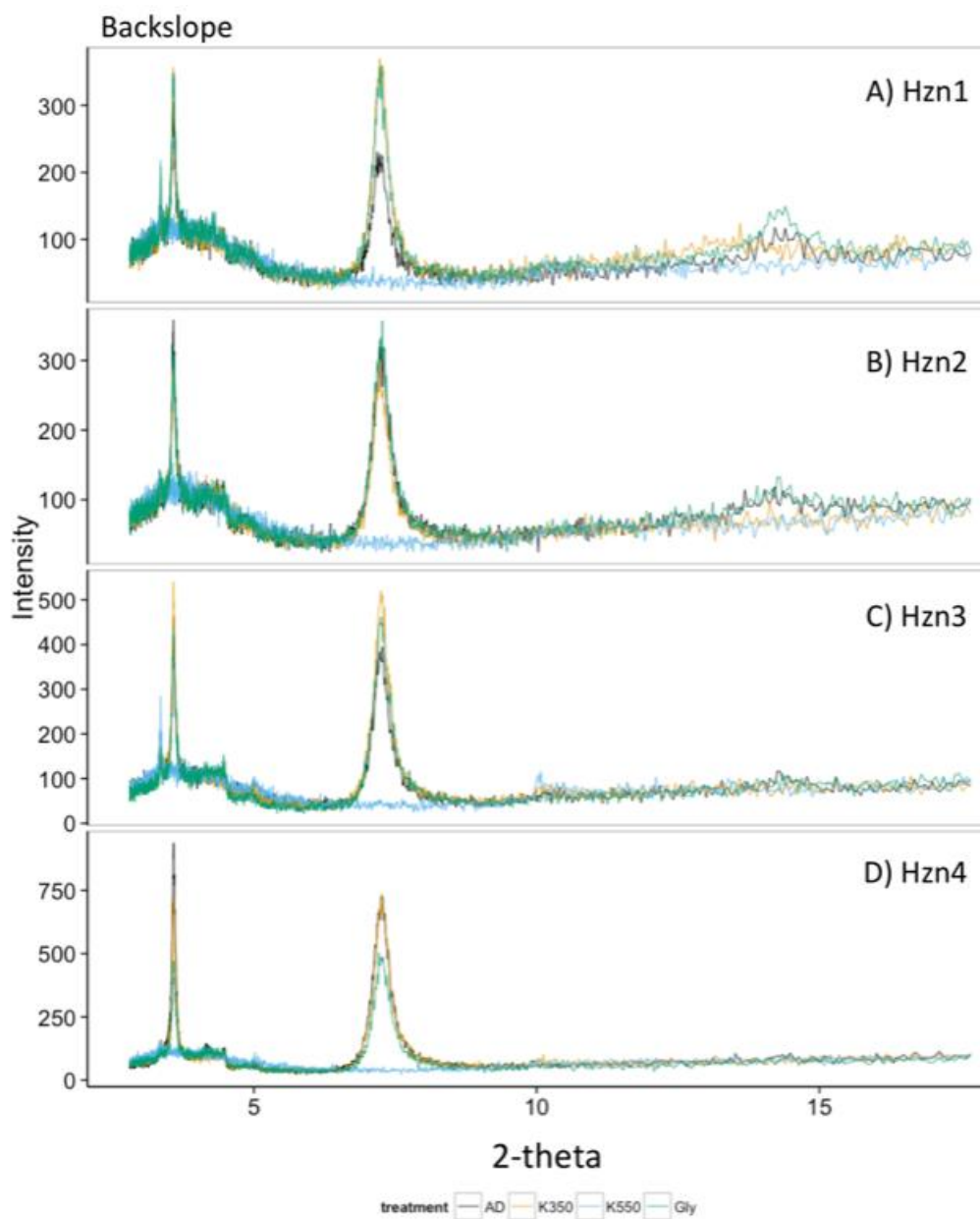


Figure E-3. X-ray diffraction diffractograms of each horizon of Pedon 3 (backslope), representing primary clay mineralogy of kaolinite.

Pedon 4

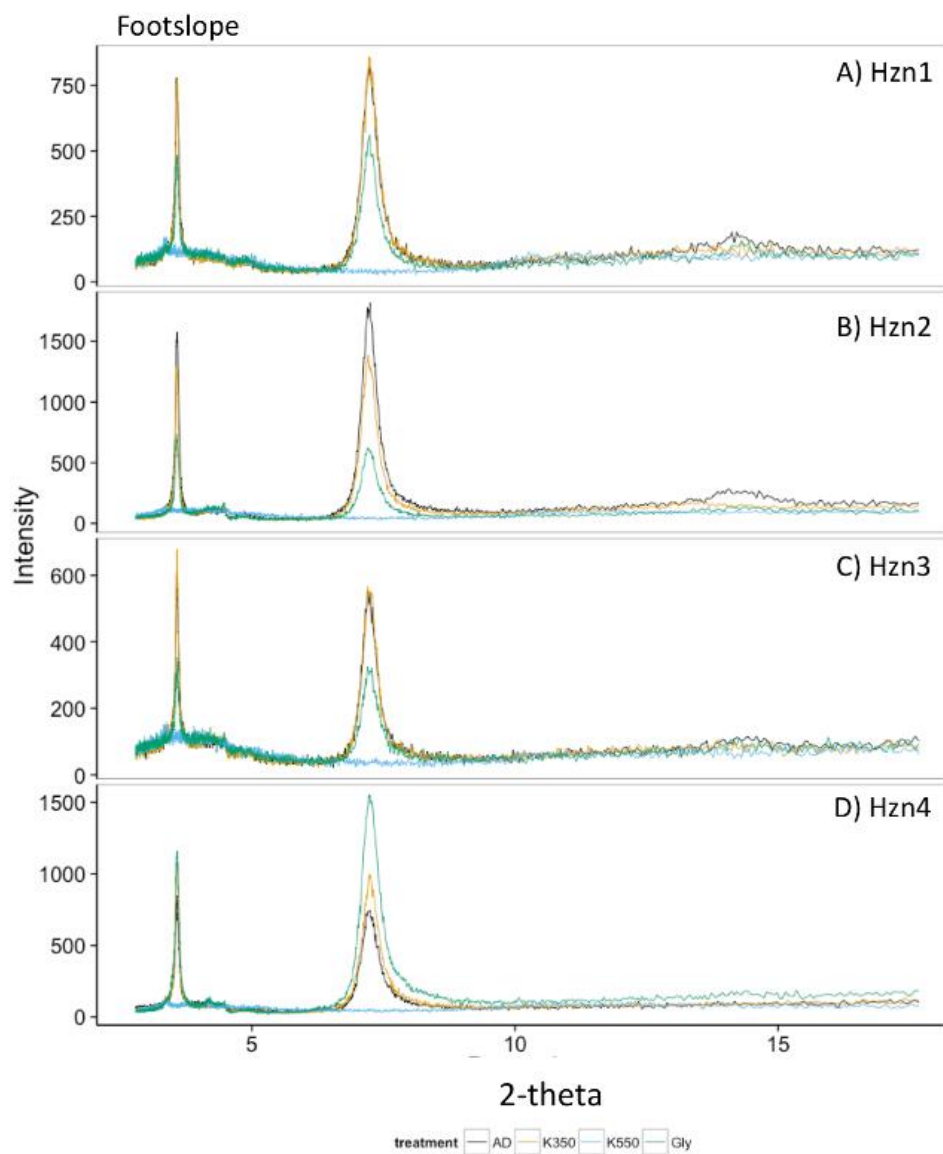


Figure E-4. X-ray diffraction diffractograms of each horizon of Pedon 4 (footslope), representing primary clay mineralogy of kaolinite.

Pedon 5

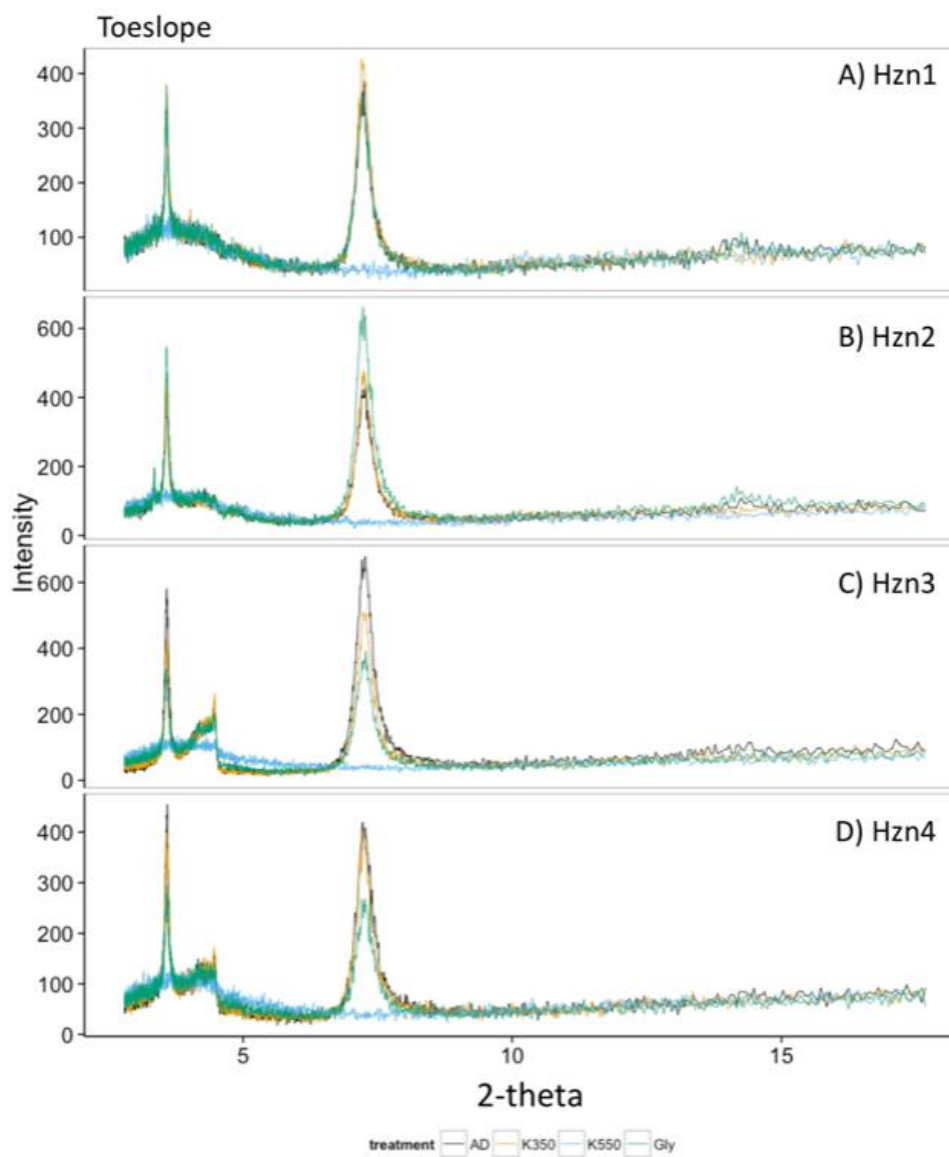


Figure E-5. X-ray diffraction diffractograms of each horizon of Pedon 5 (toeslope), representing primary clay mineralogy of kaolinite.

Pedon 6

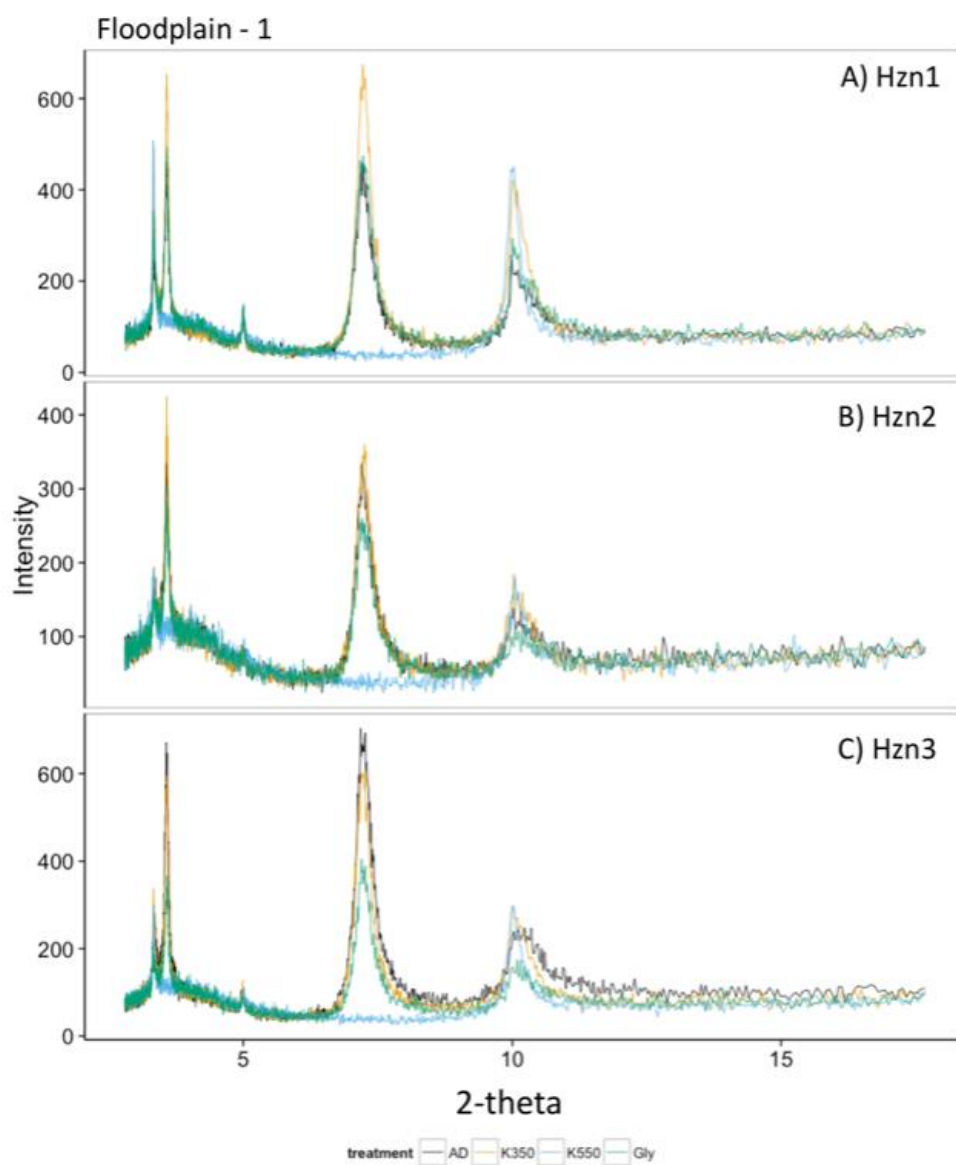


Figure E-6. X-ray diffraction diffractograms of each horizon of Pedon 6 (floodplain - 1), representing primary clay mineralogy of kaolinite and illite.

Pedon 7

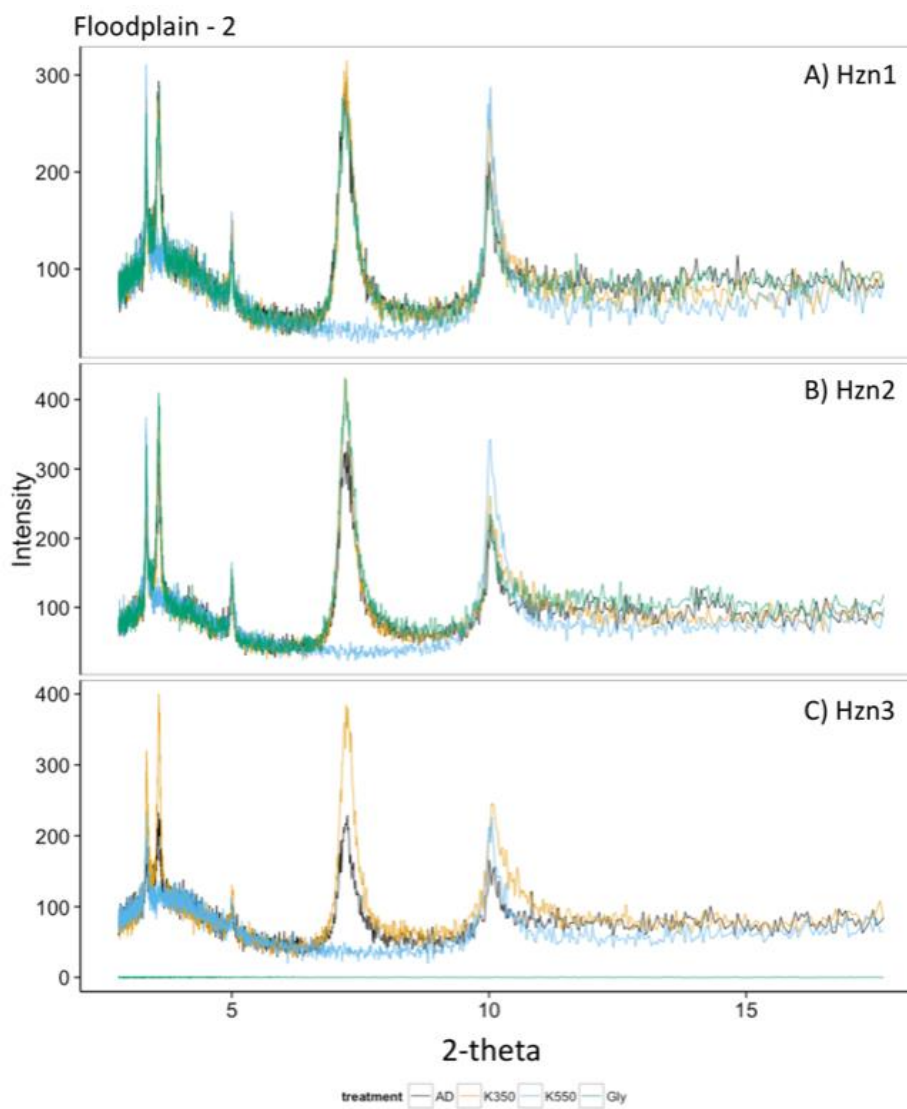


Figure E-7. X-ray diffraction diffractograms of each horizon of Pedon 6 (floodplain - 1), representing primary clay mineralogy of kaolinite and illite.

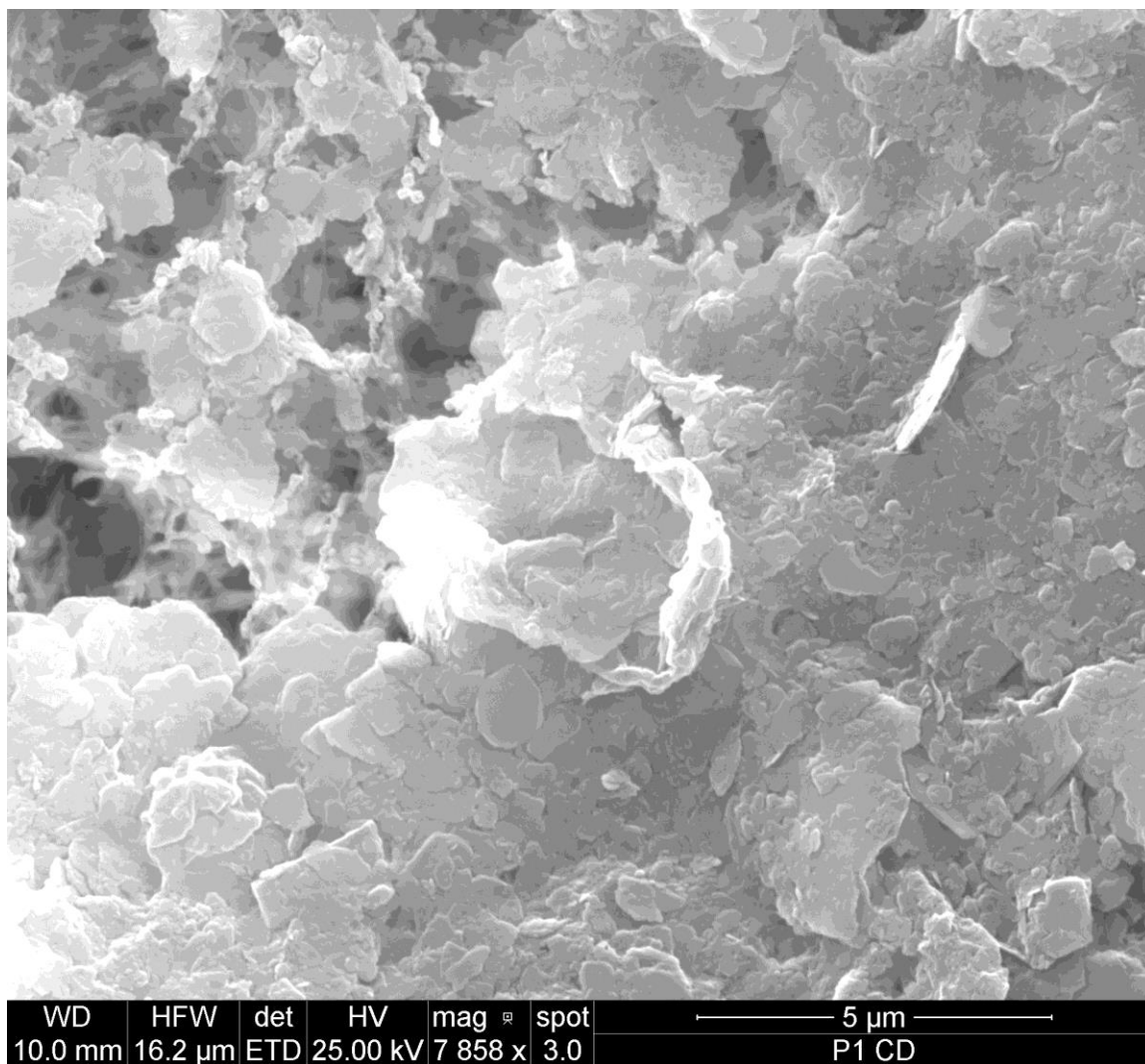
APPENDIX F: SCANNING ELECTRON MICROSCOPE PHOTOMICROGRAPHS
PLATES

Figure F-1. Pedon 1, A horizon (summit, 0-9 cm), Clay particle size image showing platy morphology of well-rounded to angular kaolinite clays, interbedded with honeycomb micro-structure in the upper left-hand corner.

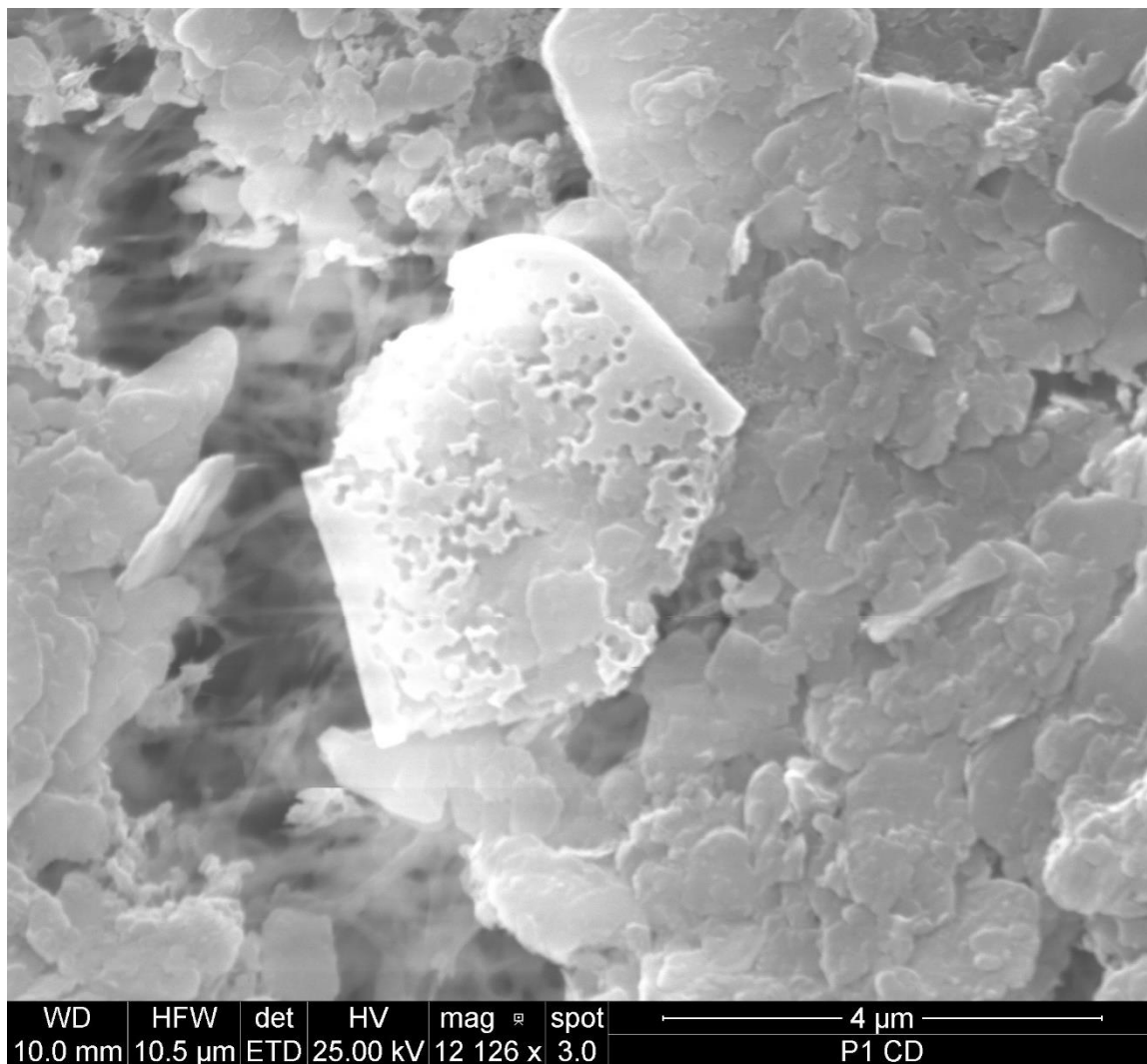


Figure F-2. Pedon 1, A horizon (summit, 0-9 cm), Clay particle size image showing platy morphology of well-rounded to angular kaolinite clays, interbedded with honeycomb micro-structure. Centered in the middle is possibly a highly weathered, dissolution pitted, platy kaolinite clay?

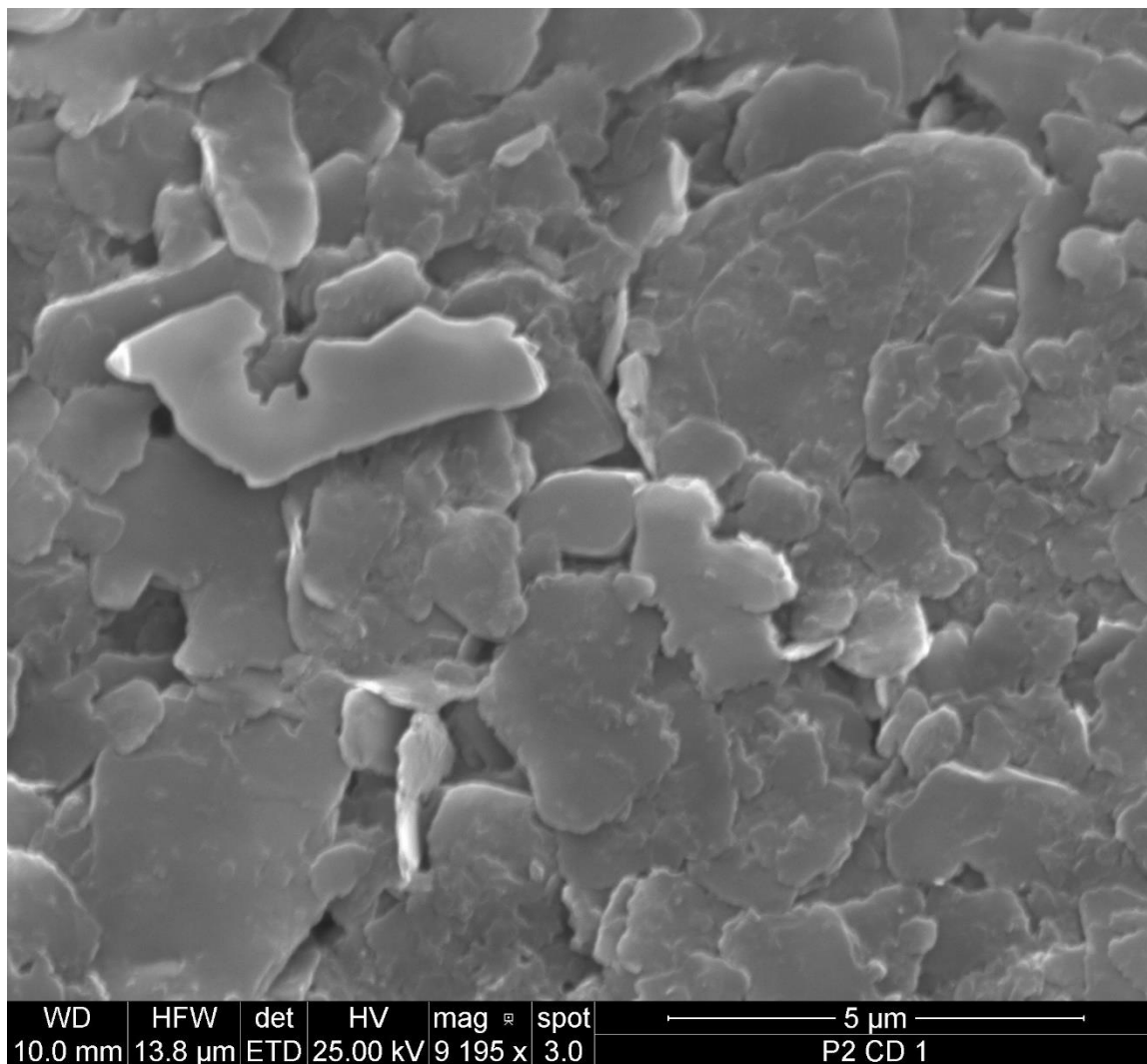


Figure F-3. Pedon 2, A horizon (shoulder, 0-24 cm), Clay particle size image showing platy morphology of possible well-rounded to angular kaolinite clays.

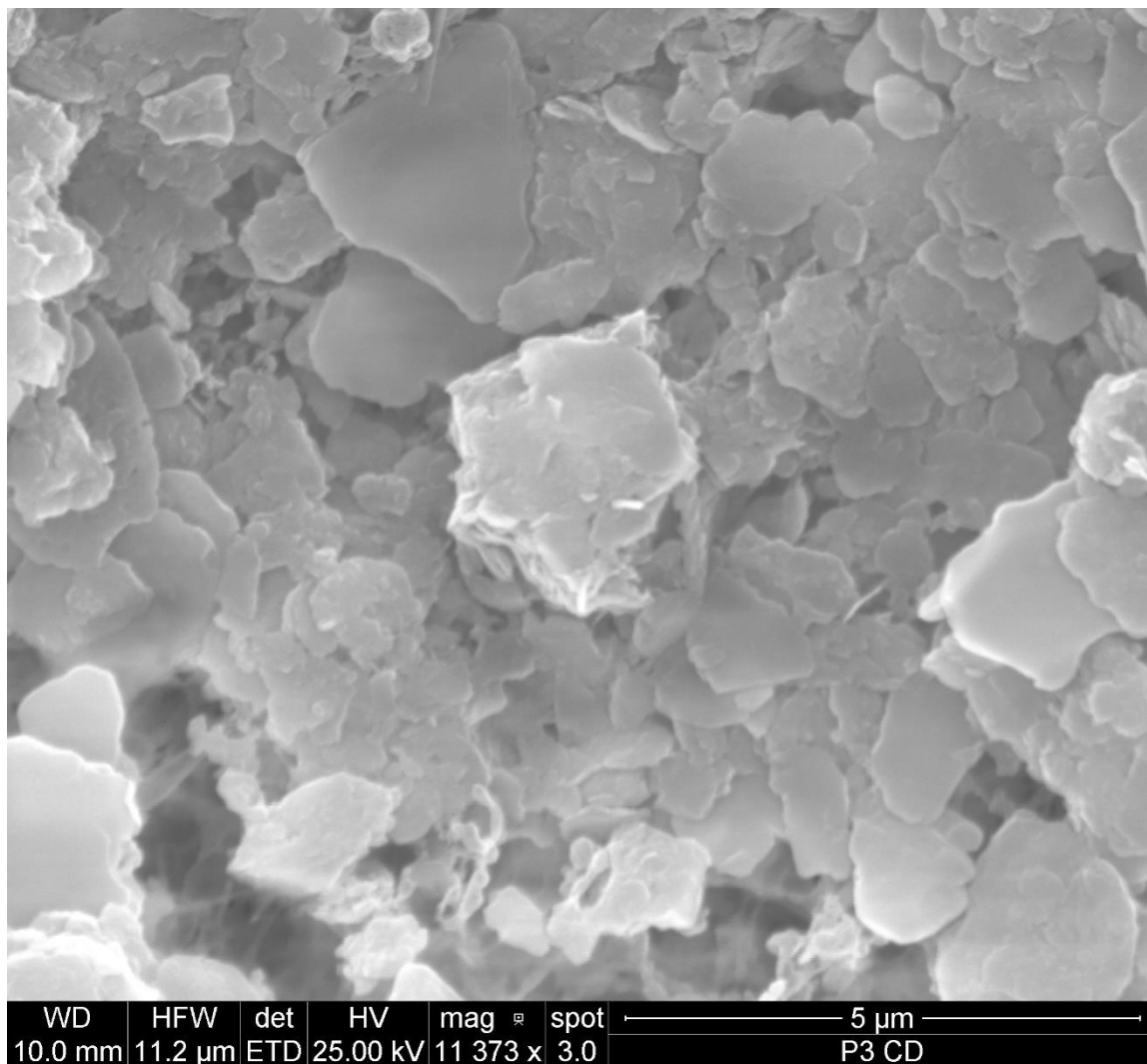


Figure F-4. Pedon 3, A horizon (backslope, 0-22 cm), Clay size particle image showing platy morphology of well-rounded to angular kaolinite clays, interbedded with honeycomb micro-structure.

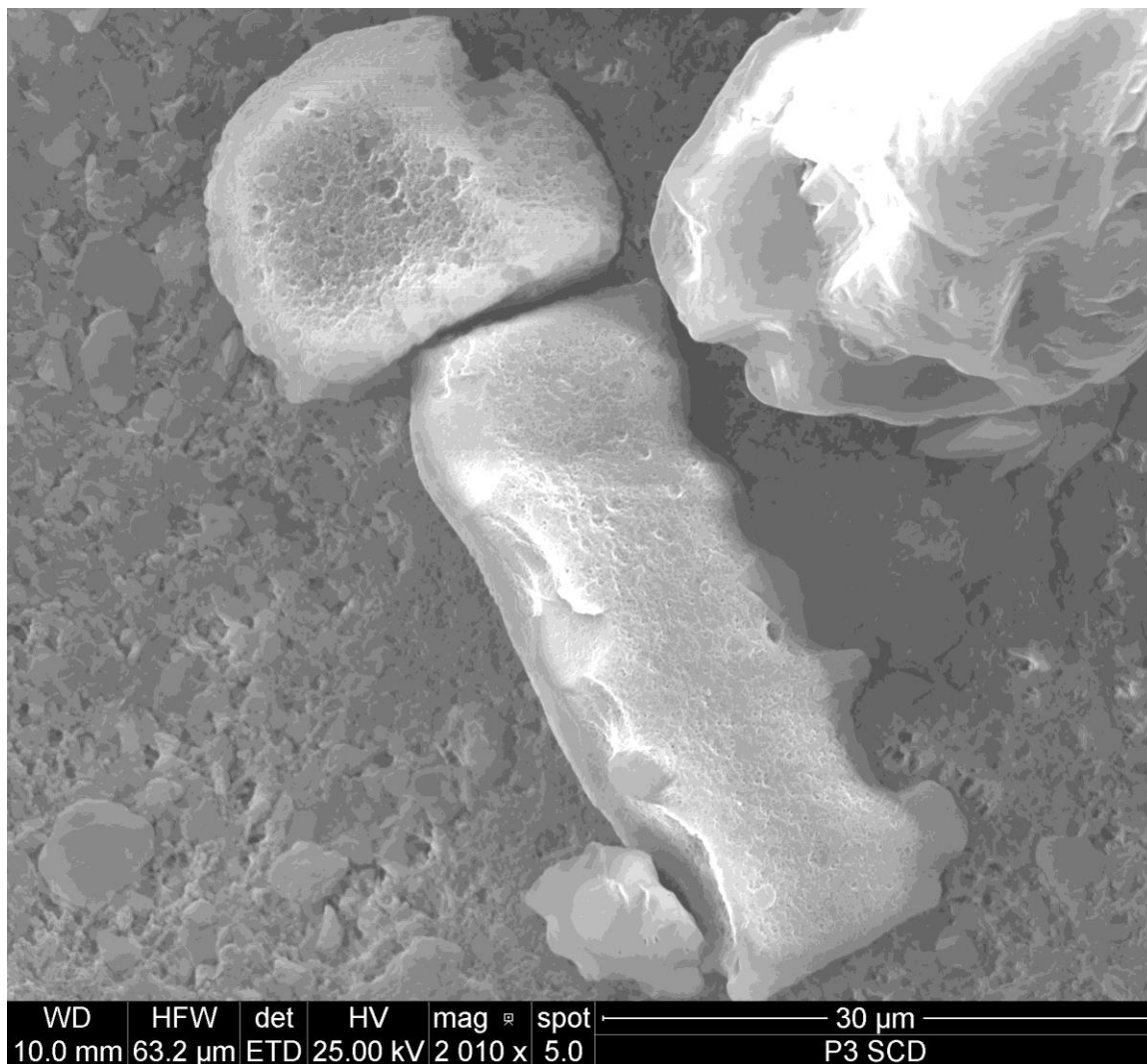


Figure F-5. Pedon 3, A horizon (backslope, 0-22 cm), Clay and silt size particle image, centered in the figure are four silt size quartz (?) grains, well rounded to angular, with sharp corners and edges, and seems to show some conchoidal fractures. Grains is sitting on a matrix of kaolinite clay particles interbedded in a honeycomb micro-structure.

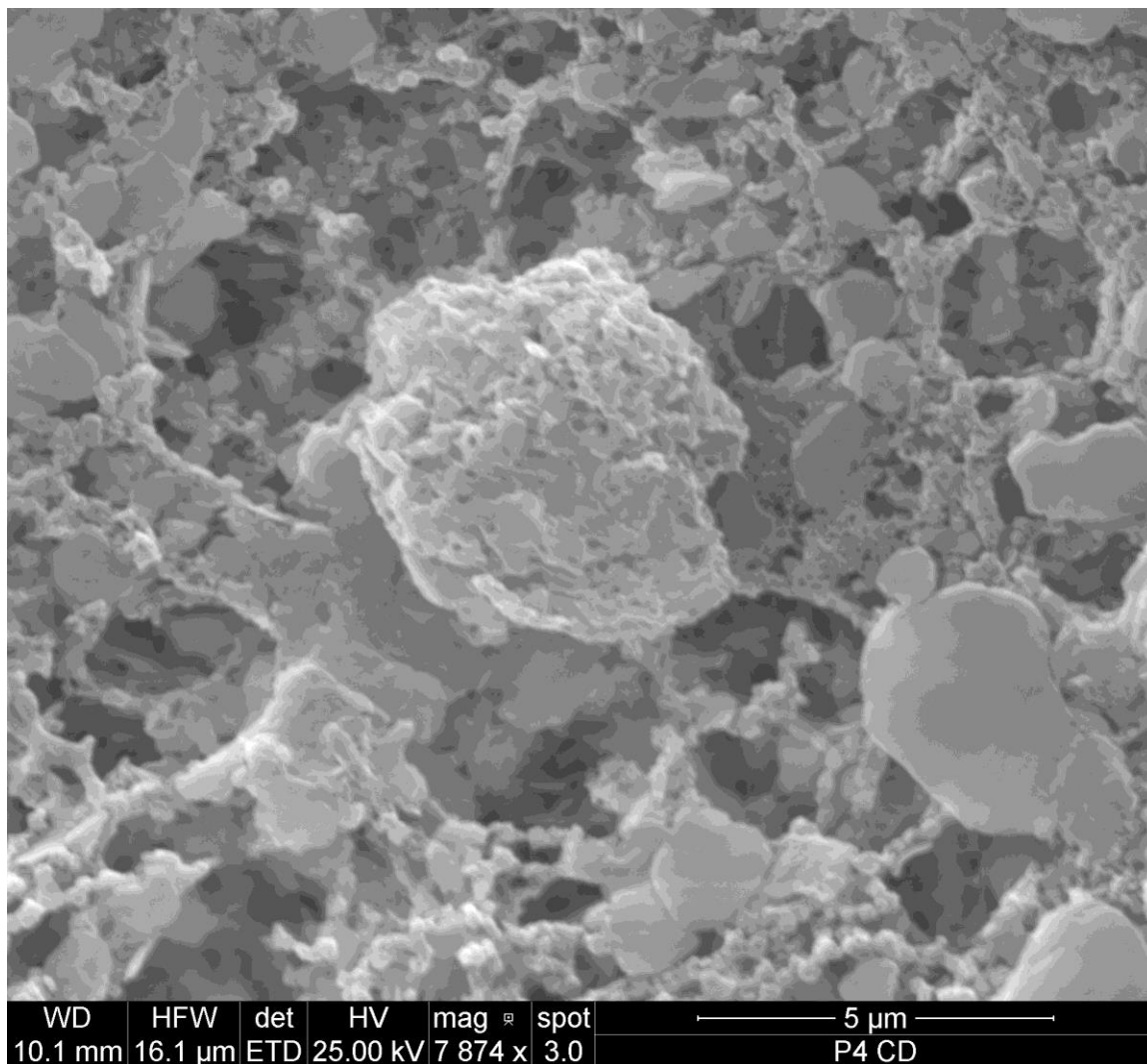


Figure F-6. Pedon 4, A horizon (foot slope, 0-6 cm), Clay size particle image showing platy morphology of well-rounded kaolinite clays interbedded with honeycomb microstructure.

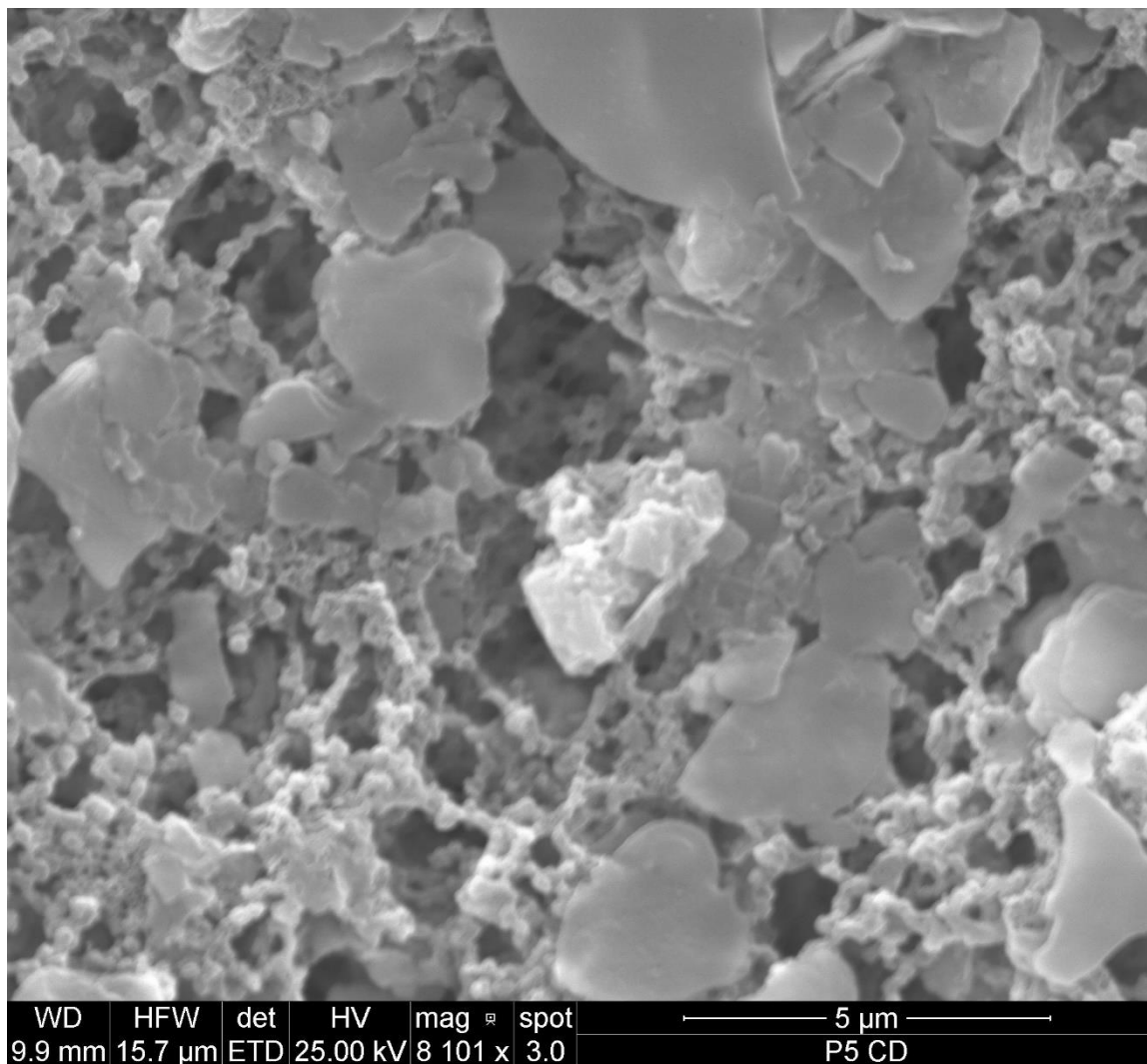


Figure F-7. Pedon 5, A horizon (toe slope, 0-9 cm), Clay size particle image showing platy morphology of well-rounded to angular kaolinite clays interbedded with honeycomb micro-structure.